

PREDICTIONS OF SIGHTING RANGE BASED UPON MEASUREMENTS OF  
TARGET AND ENVIRONMENTAL PROPERTIES

(Final Report)

Jacqueline I. Gordon

U. S. Naval Ordnance Test Station  
Contract No. NL23(60530)29657A

September 1963  
SIO Reference 63-23

## TABLE OF CONTENTS

	<u>Page</u>
1.0 SUMMARY	1
2.0 FIELD EXPERIMENT	5
2.1 Introduction	5
2.2 Range	6
2.3 Targets	11
2.4 Ground Station	13
2.5 Photographic Plane	19
2.6 Observation Plane	24
2.7 Observers	27
3.0 RESULTS	28
3.1 Introduction	28
3.2 Sighting Range Predictions	30
3.3 Recognition Predictions	35
3.4 Recommendations	37
3.4.1 Target	37
3.4.2 Contrast Transmission of the Atmosphere	39
3.4.3 Observation Plane	40
3.4.4 Observers	40
4.0 TECHNICAL DETAILS	41
4.1 Introduction	41
4.2 Field Experiment	41
4.2.1 Introduction	41
4.2.2 Range	41
4.2.3 Targets	42
4.2.4 Ground Station	45
4.2.5 Photographic Plane	51
4.2.6 Observation Plane	60
4.2.7 Observers	64
4.3 Sighting Range Predictions	64
4.3.1 Computer Program	64
4.3.2 Calculation of Sighting Range	68
4.4 Predictions of Recognition	80
4.4.1 Computer Program	80
4.4.2 Recognition Calculations	82
5.0 ACKNOWLEDGMENTS	86
6.0 REFERENCES	87

## 1.0 SUMMARY

During the summer of 1962 a field experiment was conducted at the U. S. Naval Ordnance Test Station, China Lake, California. This field test consisted of a coordinated program of visual sightings and measurements of the environmental and target properties appropriate to the observations. The specific task undertaken by the Visibility Laboratory was to aid in the design of the experiment to obtain the observations, to conduct the program of measurement of the environmental and target properties, and to use these data to predict the sighting ranges.

This report will contain a description of the design of the visual experiment, the details of the program of geophysical measurement, and the predicted sighting ranges. The observed sighting and recognition ranges will be published in a separate report by the Naval Ordnance Test Station.<sup>1</sup>

The site of the visual experiment was a long, flat, bulldozed strip oriented north-south on "Charlie" Range at China Lake. The observers were experienced naval pilots. The two targets were a Sherman tank and a radar van. The pilots were instructed to fly north at a speed of approximately 270 knots at a set altitude and search for a vehicle parked on

the strip. Upon detection they were to determine whether the vehicle was the tank or the radar van. The accurate position of the aircraft at the point of detection and, again, of recognition was determined using the tracking facilities available at "Charlie" Range. A total of 101 sightings were made over a period of three weeks. The location in the desert made it possible to obtain clear, relatively homogeneous weather conditions for the period of the field experiment. To further restrict the variability of the environmental conditions for observations at a given altitude, the early morning flights were all flown at 1000 feet above ground level, the mid-morning flights were at 4000 feet, and the mid-day flights were at 2500 feet.

A temporary ground station was established by the Visibility Laboratory during the three weeks of the field experiment near the northern end of the bulldozed strip. During each observation flight, photographs were taken at this ground station of an accurate model of the target on the dirt, thus documenting photographically an inherent contrast map of the target and background. Concurrently with the above, photometric measurements were made of the inherent luminance of the sunlit and shadowed dirt as a function of observation angle. Also, an illuminometer and shadow intensity meter was operated to provide a measure of the similarity between days and between the various times of a given day.

Contrast transmission of the appropriate downward paths of sight was obtained with the aid of a photographic plane and camera supplied by the Naval Ordnance Test Station. The two test objects utilized as photographic targets for this part of the program were the forementioned bulldozed strip and a rectangular area which was covered with road oil expressly for this field experiment. The Visibility Laboratory ground station was located at the northeastern corner of the oiled area. During the photographic flights photometric measurements were made at the ground station of the inherent contrast of the oil against the dirt. The aerial photographs supplied the measure of apparent contrast, and the ratio of these two values yielded the contrast transmittance.

The contrast transmittance of the windscreen of the observation planes was obtained by photographing a self-luminous grey scale both through the windscreen and outside the plane while the aircraft was parked on the runway.

The sighting ranges were predicted utilizing the above measurements of target and environmental properties. The predictions of the visual response of the observer to the inherent target complex were obtained utilizing the theory, data, and computer program developed under the Visual Target Classifier Program of the Visibility Laboratory; this long-term program has been supported by the Air Force under Bureau of Ships Contracts NObs-72092 and NObs-84075. A full description of this part of the visibility prediction technique will be contained in a report soon to be prepared for the Air Force project.<sup>2</sup>

Basically, the computer program predicted responses of the observer to the inherent target complex as determined from the photographs of the models taken during the field experiment. These predictions were first modified by the combined contrast transmittance of the atmosphere and the aircraft windscreen. The result was a quantitative description of the detection lobe for all forward paths of sight, that is, the region within which a target would be detected for a series of paths of sight. These lobes were appropriate to fixations of 1/3 second in duration. The detection lobes were used as the basic tool for developing a prediction of a sighting under conditions requiring search. By assuming a systematic search pattern restricted to the areas in which the target was expected to appear, predictions of the average sighting range were made.

There were two equally probable interpretations of the relationship between visual thresholds obtained under rigorous, restricted, laboratory conditions and visual response during the search situation in the field experiment. One yielded a conservative estimate of sighting range, the other a range that might be interpreted as the best possible estimate. Both estimates are given in the following report. It was predicted that the radar van would be sighted at longer ranges than the tank at all three altitudes. Also, sighting range was predicted to increase with altitude, for the flight altitudes of 1000 feet to 4000 feet.

## 2.0 FIELD EXPERIMENT

### 2.1 Introduction

The field experiment was designed to obtain as many sightings as possible for a few restricted conditions. To simplify both the observation task and the prediction calculation, the search was restricted to a simple condition, searching for a target on a long dirt roadway. To simplify the task of obtaining the appropriate contrast transmittance data, the search was further restricted to looking forward over the nose of the aircraft.

It was desired by the Naval Ordnance Test Station to obtain data at more than one altitude and to obtain recognition distances as well as sightings. Thus there were six conditions for sightings: two targets, each at three observer altitudes. The recognition problem was defined as determination of whether the target was a tank or a radar van.

During the first week of the field experiment, 16 to 20 July 1963, the altitudes at which the observers flew were 1000, 4000, and 8000 feet during early morning, mid-morning, and mid-day respectively. It was found at that time that the 8000-foot observer could not be tracked adequately, nor were the observers detecting or recognizing the targets before the cockpit restricted their field of view forward. Thus for the final two weeks, 30 July through 10 August 1963, the observations during mid-day were made at an altitude of 2500 feet instead of 8000 feet. The bulk of the observations were made during these final two weeks.

## 2.2 Range

The physical layout of "Charlie" Range and its tracking and communication facilities were ideal for the field experiment. The long bulldozed strip, a portion of which is depicted in Fig. 1, was 80 000 feet in length. Target center, or the 0 North position, was halfway up the strip. The southern portion, 40 000 feet in all, was used to vector the pilots to the area used for the observations. The targets were placed anywhere from target center to about 26 000 North. As can be seen from the contour intervals on the map in Fig. 1, most of the area used was flat with a gradual rise toward the northern end.

The dirt strip was freshly bulldozed prior to the field experiment to remove the encroaching sage, and widened to provide a larger photographic target for the contrast transmission measurements. The surrounding sage and the large bulldozed rectangle, 1000 feet wide and 3000 feet long, at 10 000 North were used as the secondary target and background for the contrast transmission measurements at the longer ranges where the oiled section became too small in angular subtense to be used as a photographic target. The dirt strip and large bulldozed rectangle are clearly seen in the aerial photographs in Fig. 2. These photographs were taken at the three observation altitudes and were used for the contrast transmission measurements which will be described in a later section. The photograph taken at 4000 feet also clearly shows the circular



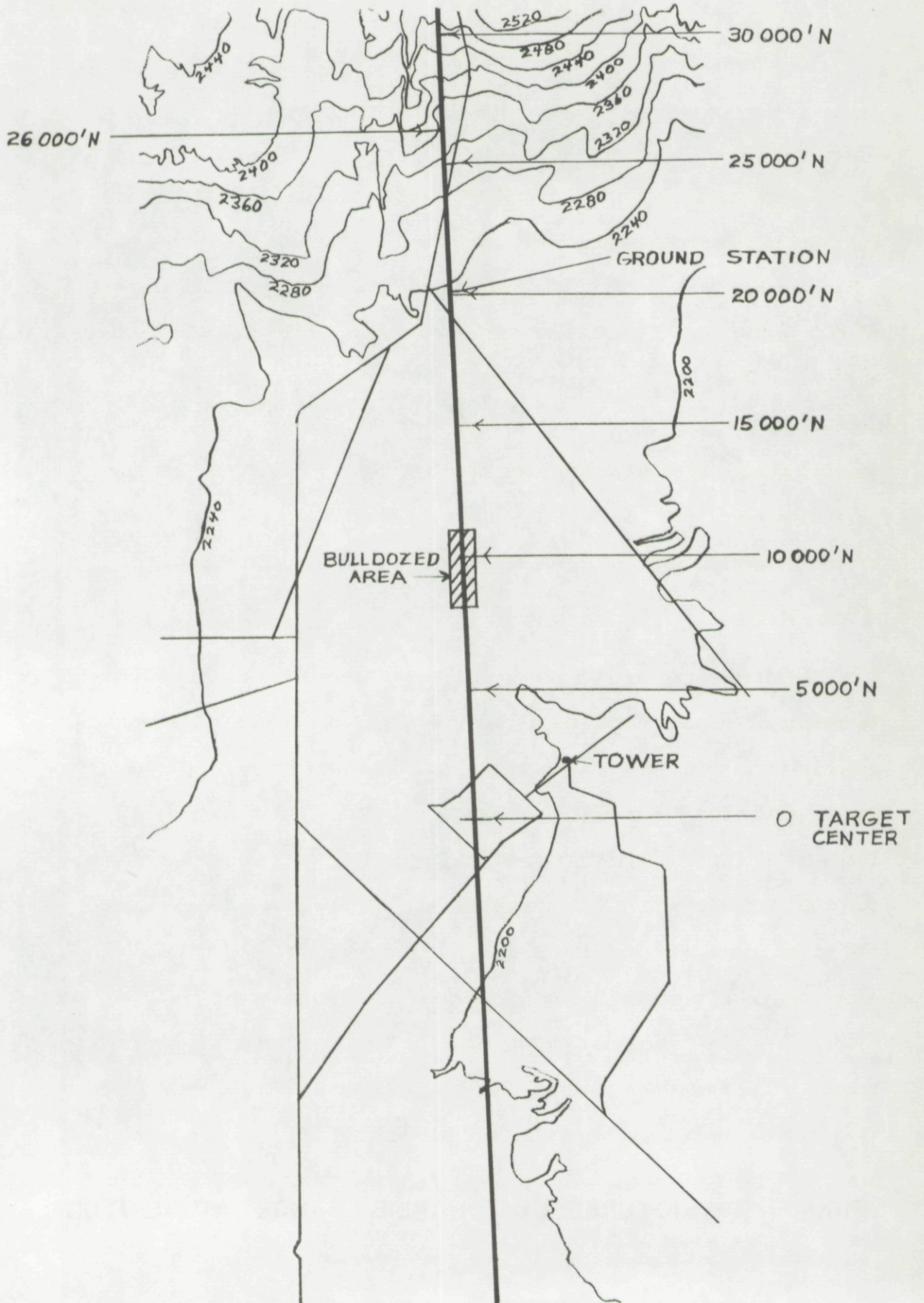
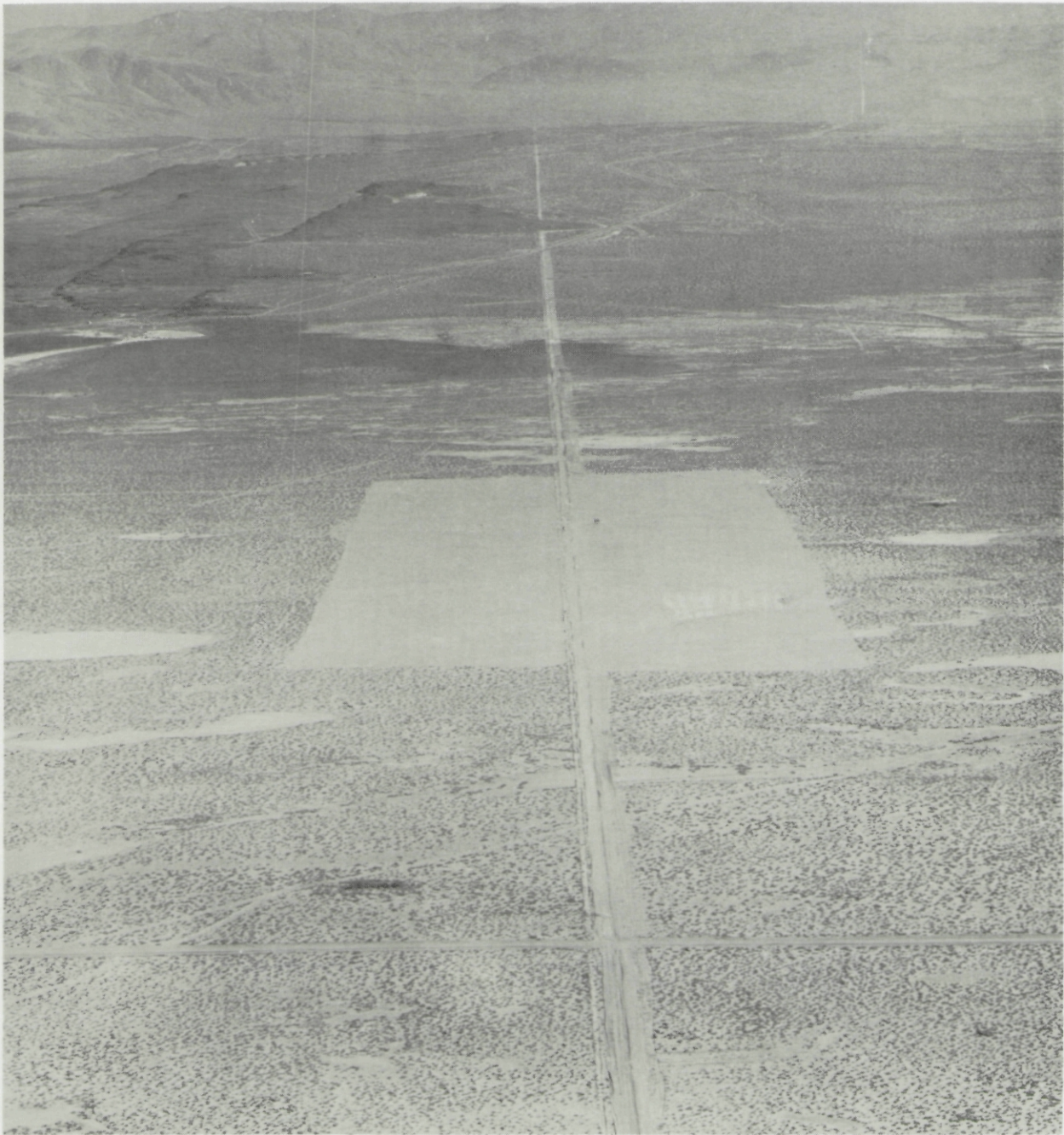
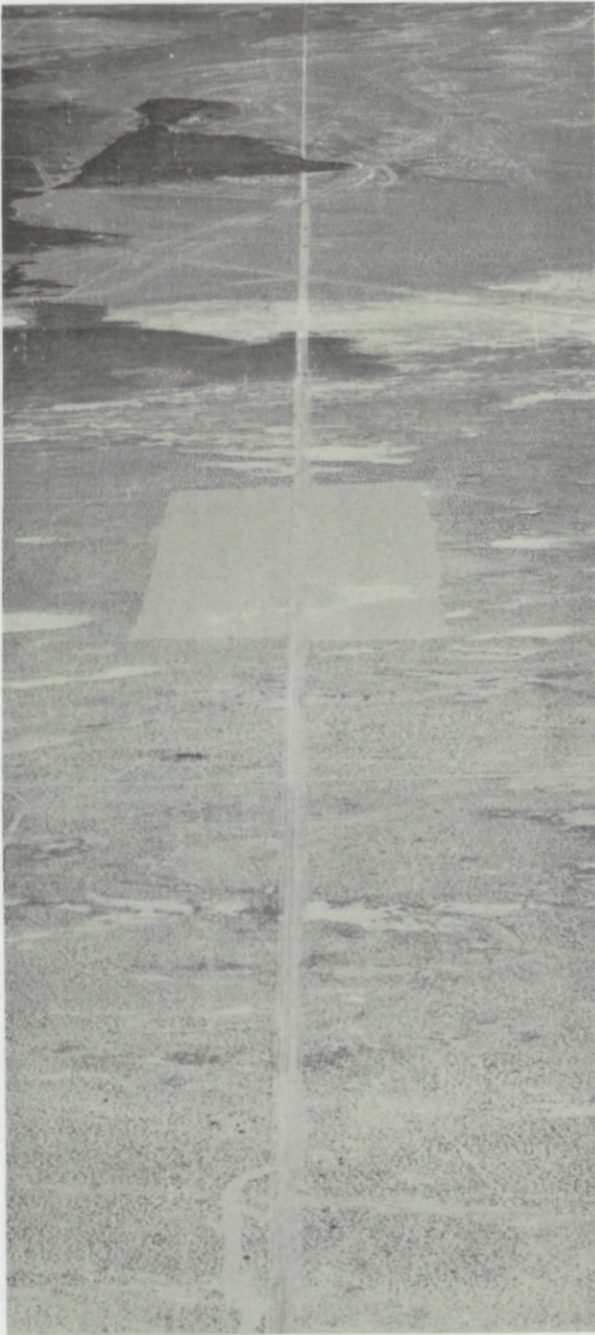


FIGURE 1 "CHARLIE" RANGE



1000 FEET

FIGURE 2 - PICTURES OF "CHARLIE" RANGE AT ALTITUDE



2500 FEET



4000 FEET

bombing target at the 0 North position. The interruption in the bulldozed strip by a blacker intrusion occurs about 26 000 North. No targets were placed beyond this point.

The tracking facilities at "Charlie" Range were used to obtain the altitude and horizontal position along the dirt strip of the observing plane during an observation run. The range control tower was in constant communication with the pilots. Tower personnel briefed the pilots on the purpose of the run, alerted by radio the Visibility Laboratory personnel at the ground station, and tracked the flight down the bulldozed strip. Range personnel also either repositioned the target or changed to a new target at the end of each day of the field experiment. In addition to the above, wind velocity data for the three weeks of the experiment were supplied to the Visibility Laboratory for use in converting indicated air speed of the observation planes to ground speed.

### 2.3 Targets

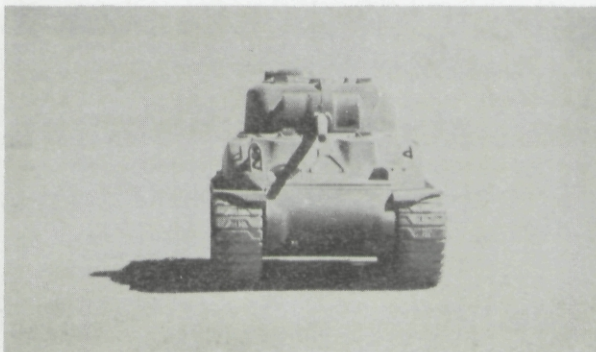
The two targets were the M4A3 Tank (76 mm Sherman Tank) and the SCR-584 Radar Van. Both were freshly painted prior to the field experiment with Army olive drab paint. Moving them into position on the dirt strip provided them with a light covering of dust. The tank was always placed facing south, whereas the radar van was faced north as shown in Fig. 3. The tank picture was taken on the first day of the observations. The dust had not reached up to the gun turret which is still shiny with the new paint. This was remedied the next day so that the whole target was evenly covered with dust.

Information on the inherent target contrast was obtained by the Visibility Laboratory through the use of models of these two targets. These models were freshly painted with a sample of the same paint, and dusted on site in a comparable fashion. A comparison between the real targets and the models can be made by means of the photographs in Fig. 3.

The appearance of the targets at the paths of sight appropriate to the forward view from an airplane is illustrated in the central column of pictures in Figs. 4 and 5. These photographs were taken of the target models during an actual 4000-foot observation run, by the Visibility Laboratory personnel at the ground station. They represent the average time of day for the 4000-foot flights.



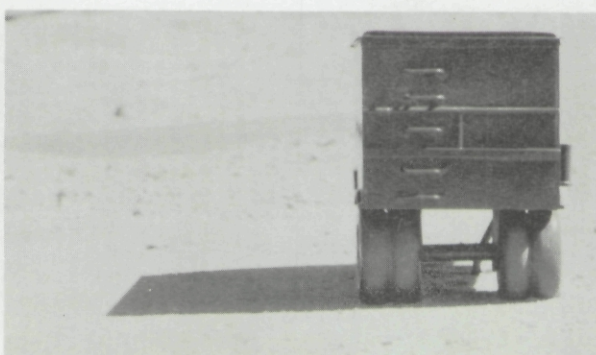
TANK



MODEL



RADAR VAN



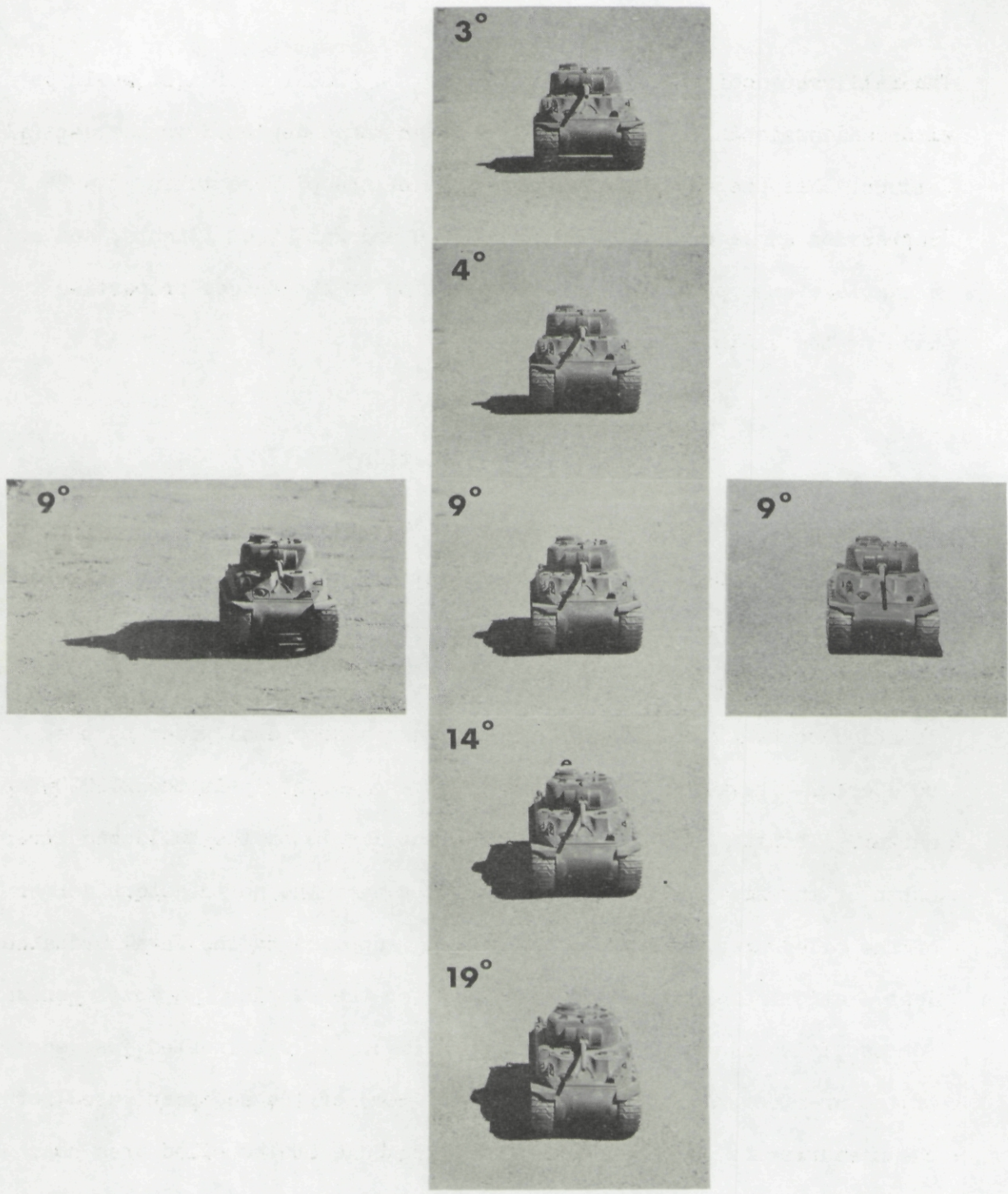
MODEL

FIGURE 3 - PICTURES OF TARGETS AND MODELS

The full range of target appearance for the 4000-foot flight would be with shadows both longer and shorter than those depicted in the central column. The photographs on either side of the picture taken at a 9° depression angle are typical of the 1000 and 2500-foot flights, and are a sample of the photographic documentation of the target properties made by the Visibility Laboratory.

#### 2.4 Ground Station

The ground station for measuring target and environmental properties during the field experiment was established at 20 000 N. Figure 6 is an aerial photograph of the ground station taken by the photographic plane at 100-foot altitude. The dark area is the oiled strip, originally intended to be 45 feet by 45 feet but made a good deal wider by the road crew. The billboard in front of the oiled strip is the 20 000-foot marker. The tank used as target for that day is on the bulldozed strip north of the station. The white building near the northeastern corner of the oiled area is a portable building supplied by the Naval Ordnance Test Station for housing the equipment for the station. A motor generator for supplying electricity was also provided. It was located just east of the area covered by the photograph. Some of the equipment used for the measurements is barely visible at the edge of the oiled area near the white building.



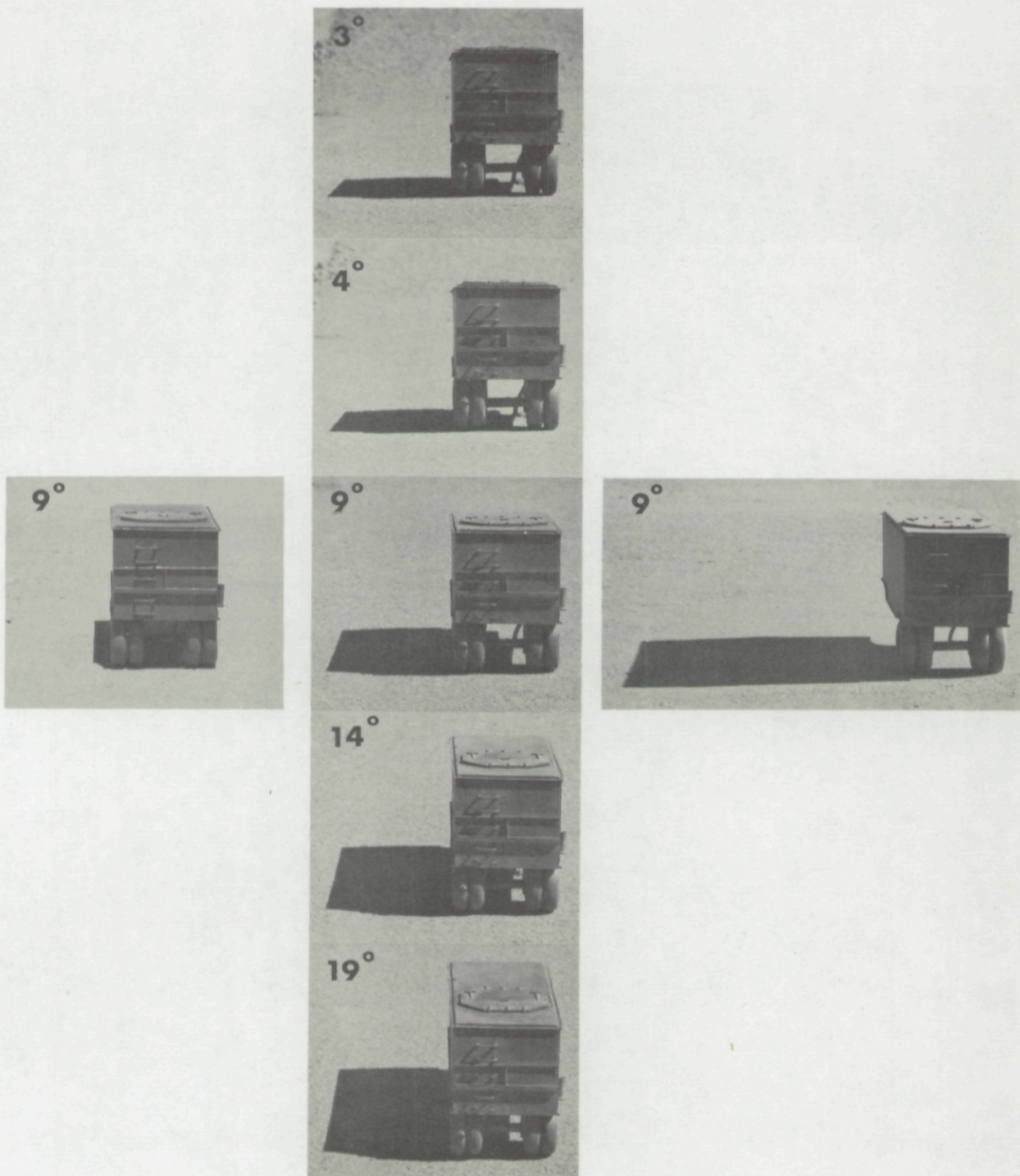
EARLY MORNING  
(Time of 1000  
ft. flights)

MID-MORNING  
(Time of 4000  
ft. flights)

MID-DAY  
(Time of 2500  
ft. flights)

FIGURE 4 - TANK MODEL





MID - DAY  
(Time of 2500  
ft. flights)

MID - MORNING  
(Time of 4000  
ft. flights)

EARLY MORNING  
(Time of 1000  
ft. flights)

FIGURE 5 - RADAR VAN MODEL



FIGURE 6 - GROUND STATION

Figure 7 is a closeup of the goniocamera and goniophotometer. The goniocamera was used to take pictures of the model of the target at various paths of sight during each observation run. This documented the inherent contrast, size, and shape characteristics of the target and its shadow against the dirt. Each filmstrip included three frames of calibrated grey scale, photographed at three different exposures. Thus the characteristic curve of the film could be fully defined and the film handled sensitometrically. Figures 4 and 5 contain pictures taken with the goniocamera.

The goniophotometer had two functions, one related to the observation runs, the other to the photographic flights. In the first case, the goniophotometer was used to document the inherent luminance of the dirt, both sunlit and shadowed, as a function of path of sight. The inherent luminance of the sunlit dirt was needed in order to compute the apparent background luminance to which the observer was adapted during the observation run. The shadowed dirt luminance was to be used to correct the photographic data from the goniocamera if the target shadow densities did not fall on a usable portion of the characteristic curve of the film. This latter correction proved unnecessary but the data were obtained as a precautionary measure.



FIGURE 7 - GONIOCAMERA (FOREGROUND) AND  
GONIOPHOTOMETER (BACKGROUND)

The goniophotometer was also used to measure the inherent luminance of the bulldozed dirt and the oiled strip as a function of angle during the photographic plane flights. This necessitated moving the goniophotometer frame back and forth between the oiled area and the dirt during these flights. These data provided the inherent contrast for a computation of contrast transmittance. The apparent contrast was obtained from photographic measurements of the oiled strip and background at altitude.

The illuminometer and shadow intensity meter was mounted on the roof of the white building. Figure 8 is a photograph of this instrument taken from on top the building. This instrument was primarily a monitoring device to provide a measure of the similarity in lighting conditions from one observation to another over the three-week period.

## 2.5 Photographic Plane

The aerial photographic coverage was for the purpose of measuring the contrast transmission of the atmosphere. The photographic plane carried beneath it a camera pod. This pod contained two cameras: one faced forward to cover paths of sight  $2^{\circ}$  to  $22.5^{\circ}$  in depression angle, the other faced vertically downward and was not used after the first week of the field experiment. Figure 9 is a photograph of the camera pod mounted beneath the plane. The forward camera, a P2V Strike camera, can be seen through the front glass window.

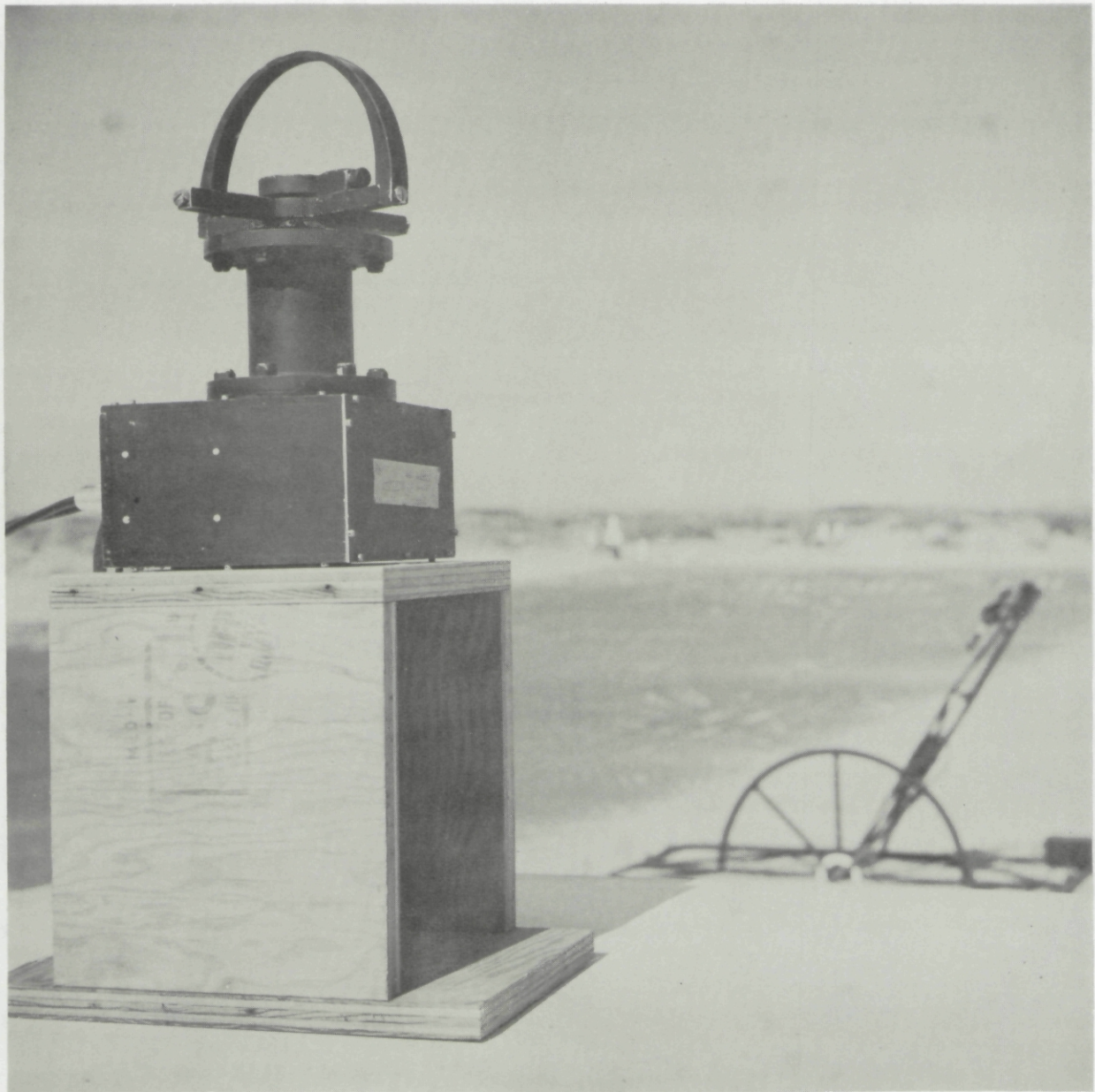


FIGURE 8 - ILLUMINOMETER AND SHADOW INTENSITY METER

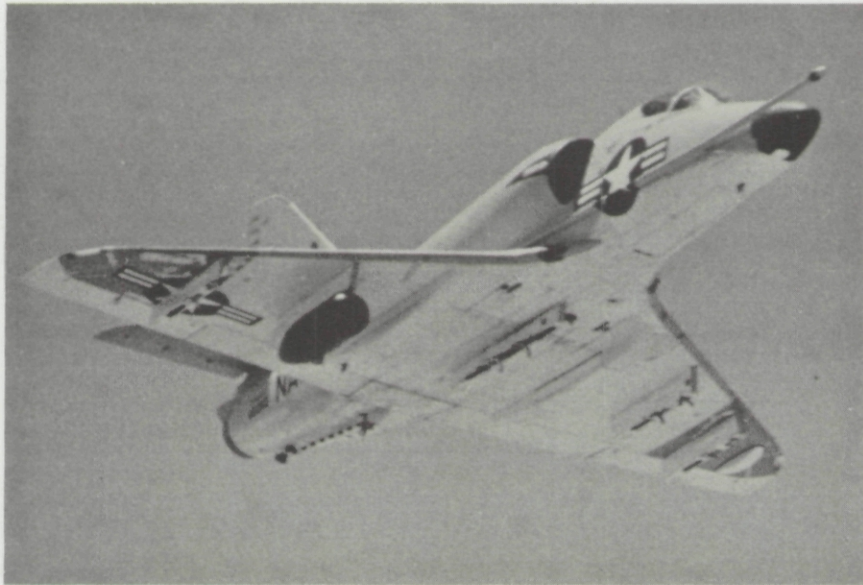


FIGURE 9 - CAMERA POD

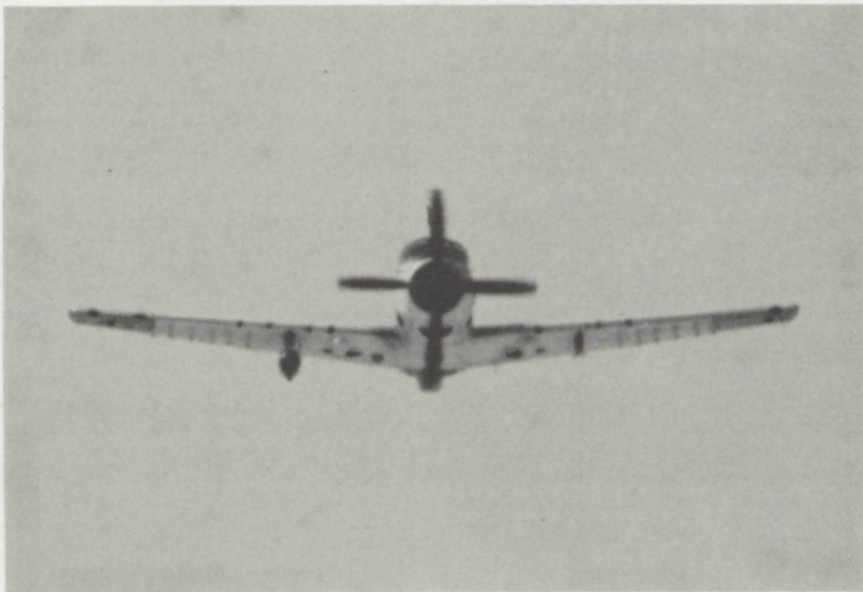
Two photographic planes were used, an A4D and an AD-5. The pod could be mounted beneath either plane. The slower AD-5 was used whenever the A4D was not available for the flights. Figure 10 contains two photographs taken from the bulldozed strip near the Ground Station. They show the two photographic planes with the camera mounted beneath as they flew past at an altitude of 100 feet.

The photographic plane flew north over the bulldozed strip on the same flight pattern as the observation planes. The basic plan was to photograph the oiled section, and the large bulldozed rectangle, at a series of depression angles of path of sight at altitudes of 100, 1000, 2500, and 4000 feet. These flights were to be made four times during the day: 1) before the first observation flight, 2) between the 1000 and 4000-foot flights, 3) between the 4000 and 2500-foot flights, and 4) after the 2500-foot flights were finished. Unfortunately this complete coverage was not possible, partially because the photographic flights constituted a sizeable interruption to the regular schedule for the range. Perfect coverage would have been attained with 46 flights; 20 were flown at appropriate times; and the films from 9 flights were usable for obtaining contrast transmittance. Thus the data on contrast transmission (presented in detail in Section 4.2.5) represent a sample appropriate to a portion of the observation runs. A bracketing of the conditions before and after a series of observations was not obtained, nor was a true average obtained of all conditions appropriate to a given target sighted from a given altitude.





**A4D**



**AD-5**

**FIGURE 10 - PHOTOGRAPHIC PLANES**

## 2.6 Observation Plane

The observers all flew in one type of aircraft which had a forward field of view  $22.5^{\circ}$  below the horizontal, if the aircraft attitude was  $0^{\circ}$ . The best information on attitude that could be obtained indicated a range of attitudes from  $+2^{\circ}$  to  $+7^{\circ}$  with a difference in attitude depending upon the altitude flown.

Figure 11 contains a photograph of the forward field of view of the observation aircraft. Unfortunately the support posts of the small instrument reflector in the center are at exactly interpupillary distance so that the pilot is forced to view through the reflector with one eye and to the side of the reflector with the other when he is searching forward. Conversation with the pilots indicated that they do not lean to one side but instead essentially ignore the presence of the reflector in looking forward.

The contrast transmission of both the view through the reflector and windscreen, and through the windscreen alone were measured photographically. A grey scale was photographed, 1) outside the plane, 2) through the windscreen, and 3) through the windscreen and reflector. The contrast transmission for six of the observation aircraft was measured with a reflection grey scale during the field test. Later a self-luminous grey scale was used and a more precise measure obtained. Figure 12 contains a picture of the self-luminous grey scale. Detailed results of these measurements are presented in Section 4.2.6.



FIGURE 11 - OBSERVER'S FIELD OF VIEW

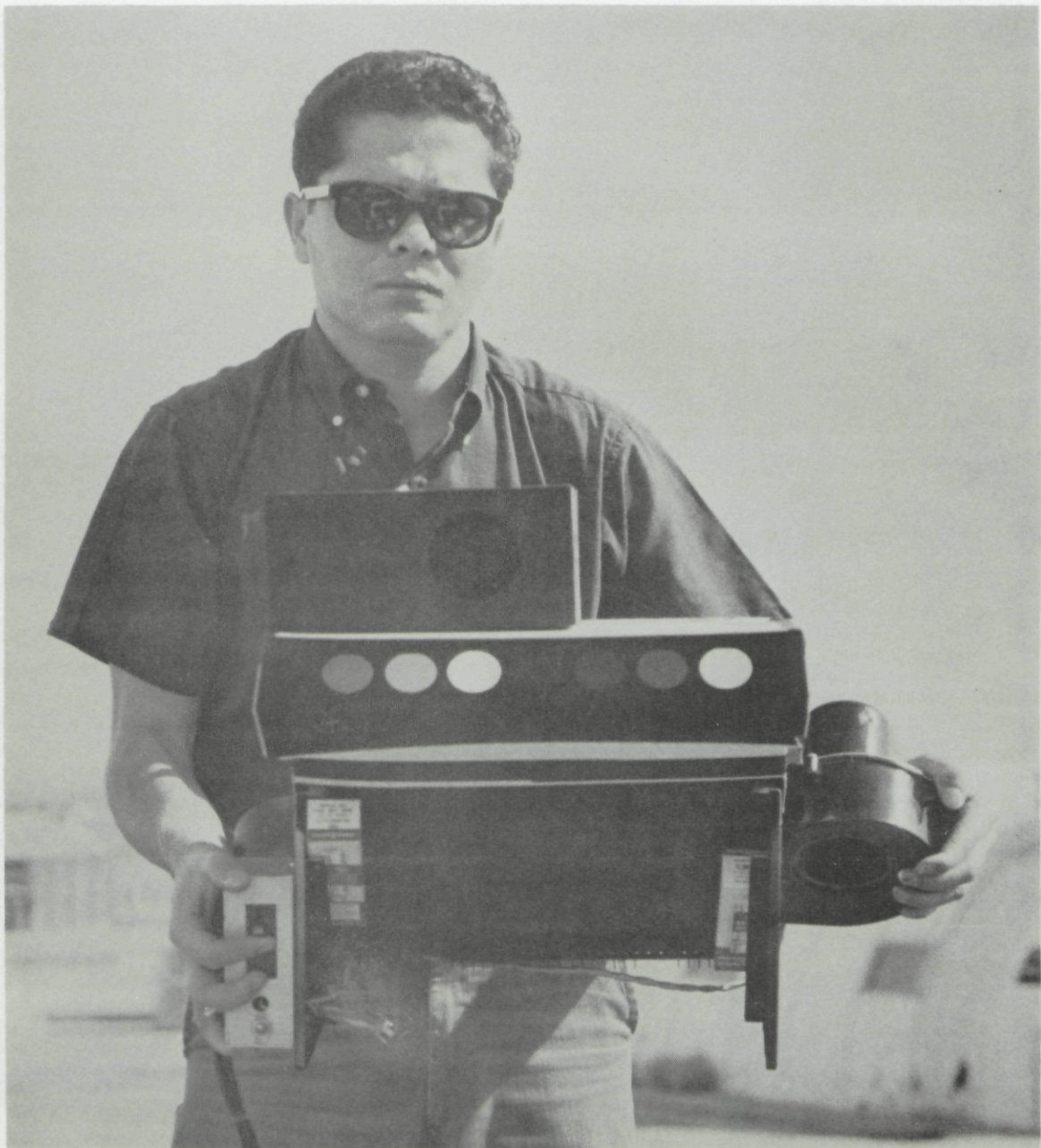


FIGURE 12 - SELF-LUMINOUS GREY SCALE

## 2.7 Observers

The observers were obtained from a squadron stationed at NOTS (VX-5) and also from visiting squadrons using the range for target practice. A pilot from VX-5 was assigned as project coordinator and he briefed all observers telling them the purpose of the flights. They were instructed to use the visors on their helmets for goggles. (The spectral transmission of one of the visors was measured at the Visibility Laboratory, see Section 4.2.7) The pilots were instructed to fly north along the bulldozed strip, to look for a tank or a radar van parked north of target center on the dirt strip, to give a signal to the range tower upon detection and another upon recognition. They were told to maintain a constant altitude and constant air speed during the flight.

Thirty-four observers participated in the field experiment, averaging three observations per pilot. Generally speaking, the results represent many observers participating in a non-repetitive experiment.

### 3.0 RESULTS

#### 3.1 Introduction

The following target and environmental property measurements were pertinent to the prediction of sighting ranges. The data from the illuminometer and shadow intensity meter indicated reasonable consistency in the atmospheric conditions over the period of the three-week field experiment. Thus similar consistency would be expected in the rest of the target and environmental property measurements. Hence the approach was to make the predictions using the average and/or median data for each target-altitude case. The inherent contrast was obtained from a single set of pictures for each case, these sets representing the median time for observations at each altitude. The contrast transmittance of the atmosphere for each altitude was an average of all data available appropriate to that altitude. (No attempt was made to separate these data with respect to which target had been used on the days of measurements since so little data had been available overall.) The contrast transmittance of the windscreen of the observation plane was very little different from the contrast transmittance through the reflector and the windscreen; also, no significant difference between the data for different times of the day could be discerned; therefore an average value of contrast transmittance was used. The range of apparent background luminances was indicated by the range of the inherent background luminance data from the goniophotometer measurements. An indication of the level of the apparent background

luminance was obtained by assuming it would be slightly greater than the inherent background luminance times the photopic transmittance of the visors used by the pilots.

The visual threshold measurements, judged to be pertinent to the problem, were for 1/3 second glimpse times with a background luminance, to which the observer is fully adapted, of 75 foot-lamberts. This included data for both the fovea and the periphery.<sup>3</sup> The 1/3 second glimpse times are appropriate to a free search situation<sup>4</sup> such as the search conditions prevailing during the field experiment. The contrast thresholds measured at a background level of 75 foot-lamberts are appropriate to the wide range of apparent background luminances indicated by the measurements noted above. At this level of background luminance, contrast threshold is nearly invariant with background luminance. It is only at much higher levels that glare reduces the contrast sensitivity of the eye. The goggles used by the pilots acted to eliminate this potential glare problem. The visual data for both the fovea and periphery were necessary in order to be able to define the detection lobes appropriate to the search problem.

In defining the detection lobes, the "hardshell" concept was used. This means that a sharply bounded region was defined within which the target would always be detected. The shape of the lobes depended upon the target and upon the altitude of the observer. In defining the probabilities of detection using these lobes, it was assumed that the observer would be systematic in the sense that he would limit his search to the area in which the target was expected to be placed, and

would not look in areas in which the target would be too distant to be detectable. The details of the method used in determining the predicted sighting ranges are given in Section 4.3.

### 3.2 Sighting Range Predictions

The sighting range can be defined as the limiting distance at which the trained military observer will be aware of seeing the target under the search conditions imposed by this field experiment. The one level of uncertainty relating to this sighting range is the "field factor" to be applied in translating laboratory visual threshold data to the field situation. These thresholds are obtained under laboratory conditions of full warning, knowledge about the target shape, size, and duration, and knowledge of location of the target.

The smallest field factor normally used for predictions in military problems is 2.4, representing a level of confidence with full awareness of target presence. When there is no warning as to the exact moment the target will appear and its exact size, etc., is not known by the observer a factor of 3.6 is needed to represent the same level of full awareness of target presence. When in addition the exact location of the target in the visual field is not known, it has been suggested that a factor of 4.8 be used to obtain this same level of awareness.

It was felt that either the small (2.4) or medium (3.6) field factor would be most appropriate for predicting the responses under the circumstances of the field experiment. Therefore predictions using both assumptions were made and are presented in Fig. 13 and Table I.



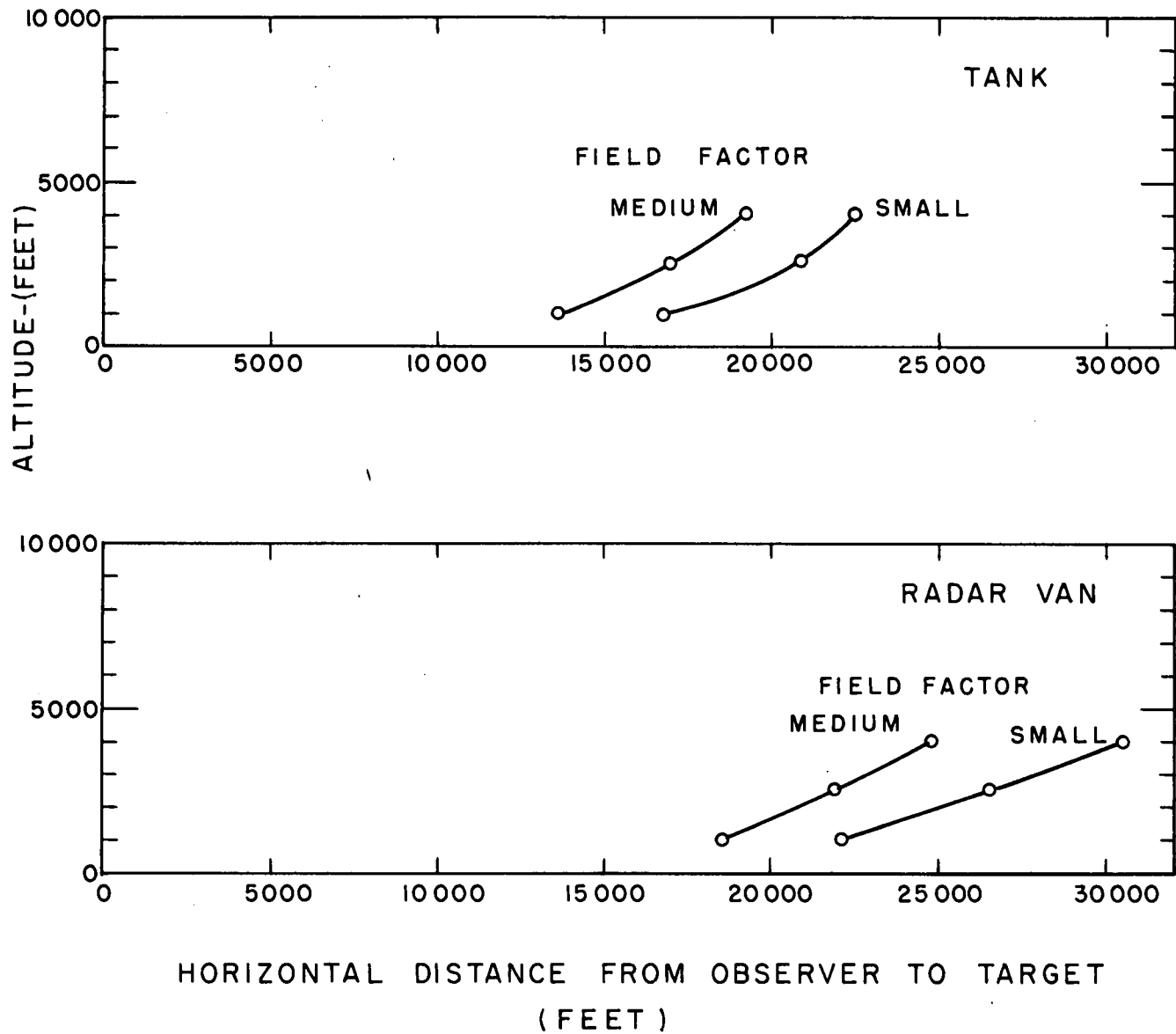


FIGURE 13 - PREDICTED AVERAGE SIGHTING DISTANCES

Table I PREDICTED SIGHTING DISTANCES FOR SYSTEMATIC SEARCH

Target	Observer Altitude (ft.) (Above Ground Level)	Average Distance (ft.)		Median Distance (ft.)	
		Field Factor		Field Factor	
		Medium (3.6)	Small (2.4)	Medium (3.6)	Small (2.4)
Tank	1000	13 600	16 800	14 000	17 100
	2500	16 900	20 800	17 100	21 000
	4000	19 200	22 400	19 500	22 800
Radar Van	1000	18 600	22 100	18 800	22 300
	2500	21 900	26 500	21 800	26 800
	4000	24 800	30 500	25 000	30 700

The average sighting distance is the prediction of the average of a number of sightings by one or more observers. The median sighting distance is that distance at which half of the observers will have sighted the target.

A fuller understanding of the meaning of the average and the median values may be attained by a glance at Fig. 14. The bar graph is the normal distribution curve and represents the percentage of the observers expected to sight the target at each observer-to-target distance. The average is the weighted sum of the distances, the weighting being represented by the bar graph. The solid curve is the cumulative probability that the target will be sighted. The median

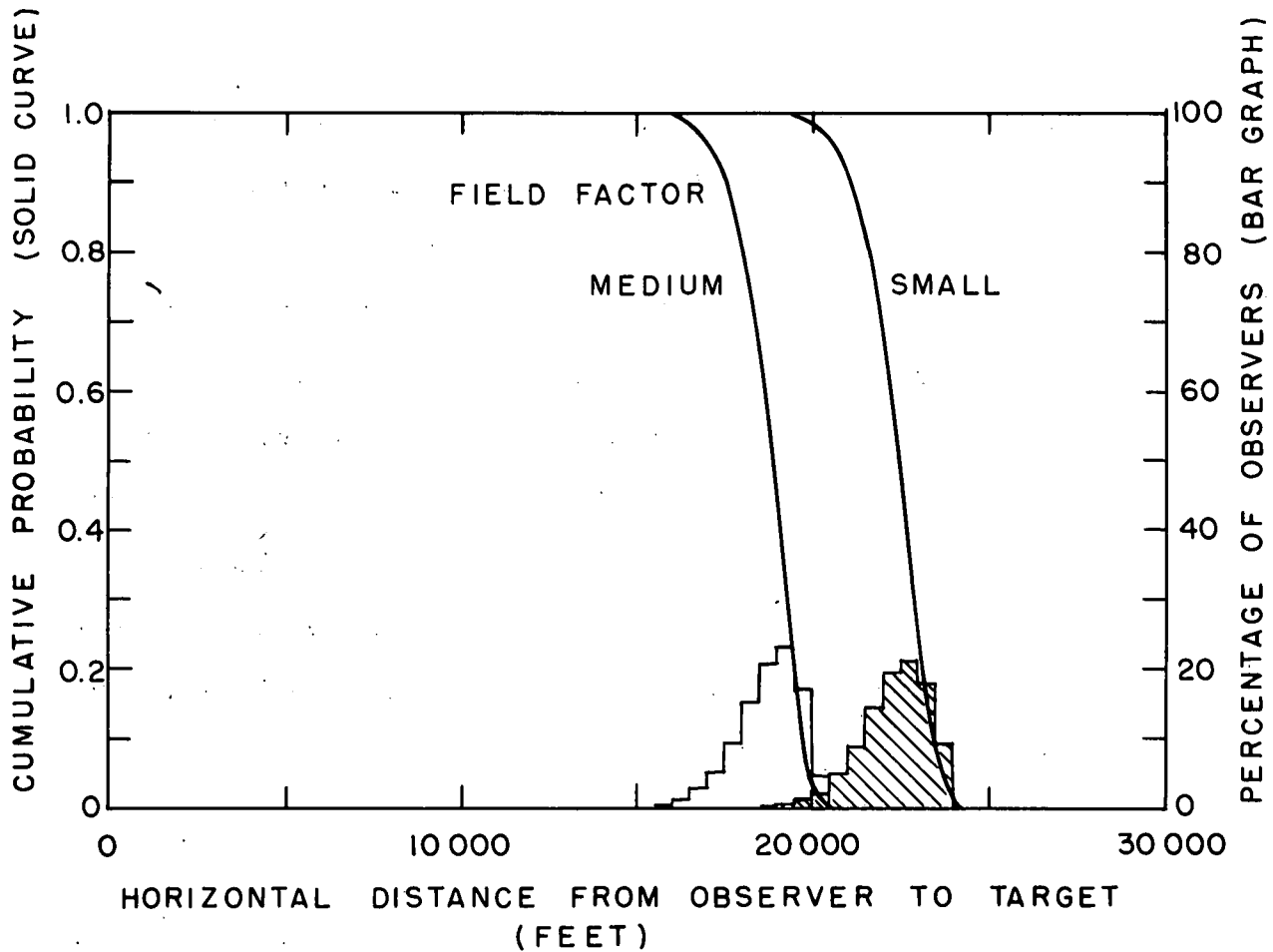


FIGURE 14-CUMULATIVE PROBABILITY CURVES AND NORMAL DISTRIBUTION BAR GRAPHS FOR SIGHTINGS OF THE RADAR VAN BY THE OBSERVER AT AN ALTITUDE OF 1000 FEET

distance is the distance corresponding to the 50 percent cumulative probability. The normal curve is skewed. The drawn out tail of the distribution toward the shorter distances accounts for the average always being less than the median distance.

The effect of using various assumptions concerning the search situation was explored for one target and one altitude: the radar van as seen from the 4000-foot observer altitude. The results are given in Table II. The choice of the appropriate field factor shows up as the most critical assumption tested. Assuming a perfectly randomized positioning of the targets on the range was very little different from weighting the results for each target position by the number of observations made for that target position. A random search, limited only to searching between 0 North and 26 000 North, was very little different from the systematic search assumed for the predictions. For more details concerning the method of computing the detection predictions refer to Section 4.3.

Table II EXAMPLE OF EFFECT OF VARIOUS ASSUMPTIONS ON SIGHTING RANGE

		TARGET: RADAR VAN	OBSERVER ALTITUDE: 4000 FEET		
Type of Search	Target Position	Field Factor	Sighting Distance (Feet)		
			Average	Median	
Systematic	Weighted	Small (2.4)	30 500	30 700	
Systematic	Weighted	Medium (3.6)	24 800	25 000	
Systematic	Weighted	Large (4.8)	21 400	21 700	
Systematic	Random	Medium (3.6)	24 700	25 000	
Random	Weighted	Medium (3.6)	24 000	24 300	

The effect of individual variability has not been adequately covered by the foregoing discussion. The probability integrals shown in Fig. 14 are of themselves an average. The visual threshold used represents an average observer based upon careful psychophysical measurements of four observers. The spread in the data for the four observers varied between a factor of 2 to 1 and 4 to 1. It has been estimated that the spread in the visual capability within the total population of "perfect" young eyes can be represented by a factor of 2 in contrast threshold in either direction. This means that the spread of the data for a large number of observers should be many times greater than that shown in Fig. 14. It also means that a measure of the relationship of the visual capabilities of the four observers to the population of "perfect" young eyes would be desirable, as would a measure of the relationship of the pilot observers to the general population of military pilots.

### 3.3 Recognition Predictions

The main task of this project was to predict detections. The theory, data, and methodology for making detection predictions is in a well-developed stage. The knowledge and methodology for making predictions of recognition distances is in a much earlier stage of development. However, since the Naval Ordnance Test Station was interested in recognition observations, an attempt was made to make a recognition prediction.

For this attempt, it was decided to establish an upper limit, i.e., to predict the longest distance at which recognition could occur. The actual recognition observations would be expected to be less than this upper limit value. No attempt was made to establish how much less than the upper limit the actual observations would be.

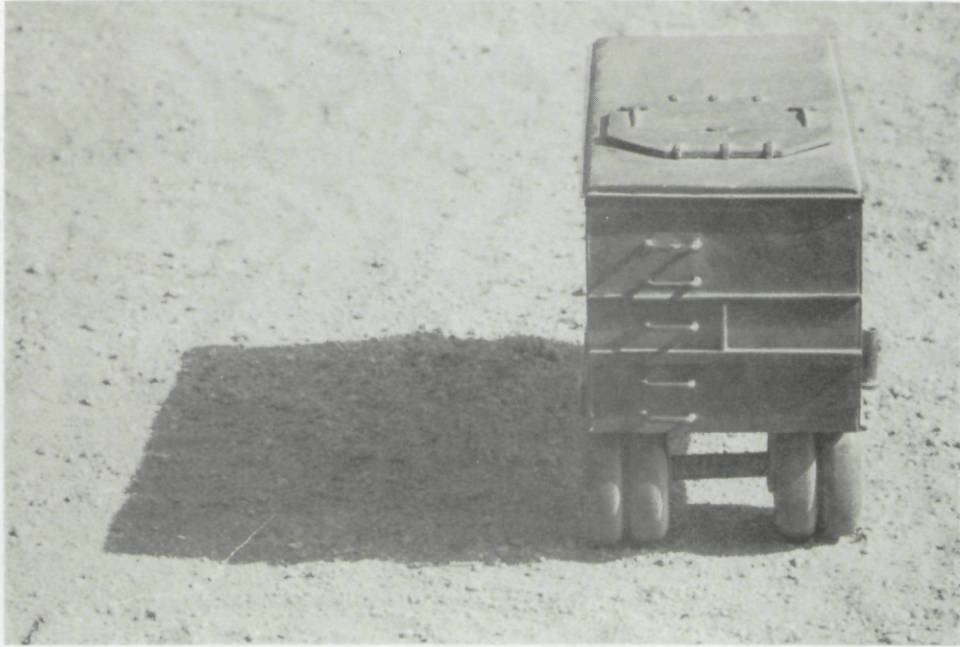
To make this prediction it was assumed that a precise knowledge of the luminance map of both targets was known by the observer at each altitude of observation and path of sight. Recognition thus could occur when the difference between the luminance maps of the two targets was capable of being detected by the observer. The observer was assumed to fixate upon the target after detection, and to recognize after both an adequate signal difference was available and after enough time had elapsed to maximize the visual threshold and to allow for cortical function. For more detail on the method of prediction refer to Section 4.4.

The end result of the prediction was that the recognition distance would be 1200 feet less than the sighting distance for each target at each altitude.

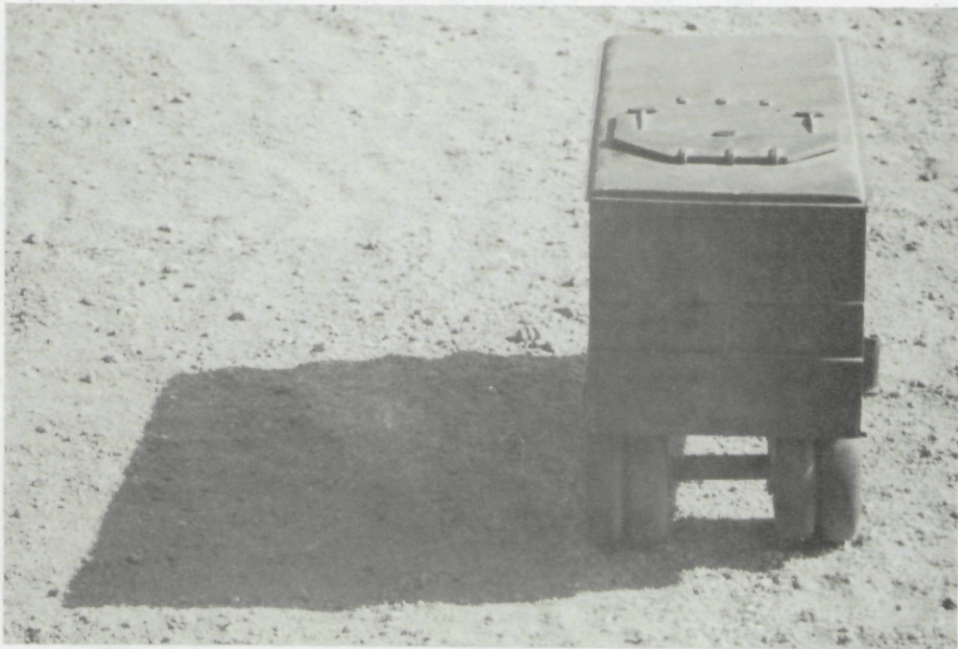
### 3.4 Recommendations

During the course of the field experiment and later during the data reduction and prediction calculations it became apparent that there were a number of sources of uncertainty that it would be desirable to eliminate should a similar field experiment be undertaken in the future. Following are a number of recommendations for eliminating these sources of uncertainty.

3.4.1 Targets. It would be desirable to document the actual position of the real target by a photograph at the time of each observation run. A direct comparison between these photographs and the model photographs would provide a measure of the accuracy of the target information obtained by use of the models. A real, though no doubt extreme, case where a slight disorientation of either model or target might lead to an erroneous documentation of target information is illustrated in the photographs in Fig. 15. These pictures were taken in the morning with the sun about  $90^{\circ}$  in azimuth; the radar van model is headed north as in the field experiment. A true north heading of the radar van yields a target with a sunlit rear end. The radar van slightly angled toward the east yields a target with a darkly shadowed rear end making a target different than the first.



RADAR VAN FACING NORTH



RADAR VAN HEADED SLIGHTLY EAST OF NORTH

FIGURE 15 - IMPORTANCE OF CORRECT TARGET INFORMATION



The real targets should be randomly changed in position and the two targets randomly interchanged at the time between altitudes of observation on each day. Thus one observer could make more than one observation per day without biasing either the detection or recognition observation.

The predictions should be made for the extreme cases as well as the median cases (beginning and end of observation period as well as median time) to obtain a measure of the effect of these differences in target information.

3.4.2 Contrast Transmission of the Atmosphere. Measurements of contrast transmission should be made before and after the observation session at each altitude. This means flights four times a day for a comparably organized experiment. In this way the change in contrast transmission over the experimental period can be measured. This was definitely not achieved in the current experiment.

Assuming the measurements would be made photographically a number of improvements would be highly desirable. The camera used should have a shutter mechanism which will operate uniformly over the frame and will reproduce exposure times to a high degree of precision. The exposure settings should be under close control so that all of the data will be on the straight line portion of the characteristic curve of the film. In this experiment much information was lost due to underexposed film and a faulty shutter mechanism.

The targets used for aerial photography should be larger and more uniform to increase the precision of the determination of contrast transmittance. If in addition, a self-luminous grey scale were photographed at the beginning and end of each roll of film, it would then be possible to recover the beam transmittance and path luminance for the appropriate paths of sight, as well as the contrast transmittance.

3.4.3 Observation Plane. It would be useful to obtain a more direct measure of plane attitude during the observation flights.

3.4.4 Observers. A more complete and carefully controlled briefing and debriefing of the observers would be desirable. (A few of the observers who did not report sightings thought the target would be out amidst the sage.) A record by the observer of which target was recognized and where would provide a double check on the observations. Interviews with the pilots concerning the method of search and the criteria used for making a recognition judgment would be of value.

A photographic documentation of the eye movements of the observer during search would be desirable.

Finally it would be extremely valuable to be able to have the pilots make some laboratory visual threshold measurements. These data would be useful in comparing the laboratory observers to the observers used in the experiment and would yield much information on individual differences.

## 4.0 TECHNICAL DETAILS

### 4.1 Introduction

The technical details concerning the field experiment are contained in the first portion of this section paralleling the organization of Section 2. The calculational details of the detection and recognition predictions are contained in the remaining two subsections, paralleling Section 3.

### 4.2 Field Experiment

4.2.1 Introduction. A description of the equipment used for the measurements of target and environmental properties and the results of these measurements will be briefly given in this section. In addition, the relationship between these data and the ensuing calculation of detection ranges will be described as appropriate.

4.2.2 Range. Tracking accuracy of the range facility was estimated to be  $\pm 25$  feet.

Wind velocity data (speed in knots and direction from true North) were supplied by the Naval Ordnance Test Station. These data were for surface to 10 000 ft. AGL (above ground level) at 1000 ft. intervals for usually five times during each day, normally at 0630, 0800, 0930, 1100 and 1220. These data were used to obtain the ground speed of the observing aircraft.

Altitude (AGL) (Feet)	Target	Indicated Air Speed (Knots)	Average Ground Speed (Knots)
1000	Radar Van	275	272
	Tank	275	272
2500	Radar Van	270	259
	Tank	270	262
4000	Radar Van	260	260
	Tank	260	260

The average ground speed was used to determine the distance traveled in one look during search.

4.2.3 Targets. The two targets were the M4A3 Tank (76 mm Sherman Tank) and the SCR-584 Radar Van.

Dimensions (feet)	Tank	Radar Van
Length	19.5	19.5
Width	8.5	8.0
Height	9.0	10.3

Both targets were freshly painted before the field experiment and coated with dust from the bulldozed strip for the experiment.

Two weeks prior to the field experiment, Visibility Laboratory personnel photographed the two targets from various aspects and were given samples of the paint for use on the models. A standard Sherman

tank model was modified slightly (hatch covers adjusted, gun barrel positioned, etc.) according to the pictures. The model of the radar van was made by the Visibility Laboratory from the pictures taken above. Both models were painted with the sample of paint provided by the Naval Ordnance Test Station. At the ground station on the bulldozed strip these models were dust coated as were the real targets.

A sample of the dirt from the bulldozed strip was brought back to the Visibility Laboratory following the field experiment. The relative spectral reflectance of this sample was measured on the Hardy Spectrophotometer, using a spectrally neutral test cell to hold the dirt in a vertical position. The flat side of the radar van model, freshly dusted with the same dirt, was also measured. Figure 16 is a graph of the data. Chromaticity coordinates, dominant wavelength and excitation purity were computed assuming Source B as illuminating source.

	<u>Dirt</u>	<u>Radar Van Model</u>
Chromaticity Coordinates x	0.370	0.352
y	0.361	0.350
z	0.269	0.297
Dominant Wavelength (m $\mu$ )	586.	496.
Excitation Purity (°/o)	10.	2.1

There is no significant color difference between the target and background. Therefore the targets were treated as neutral in color and contrast solely based upon luminance differences.

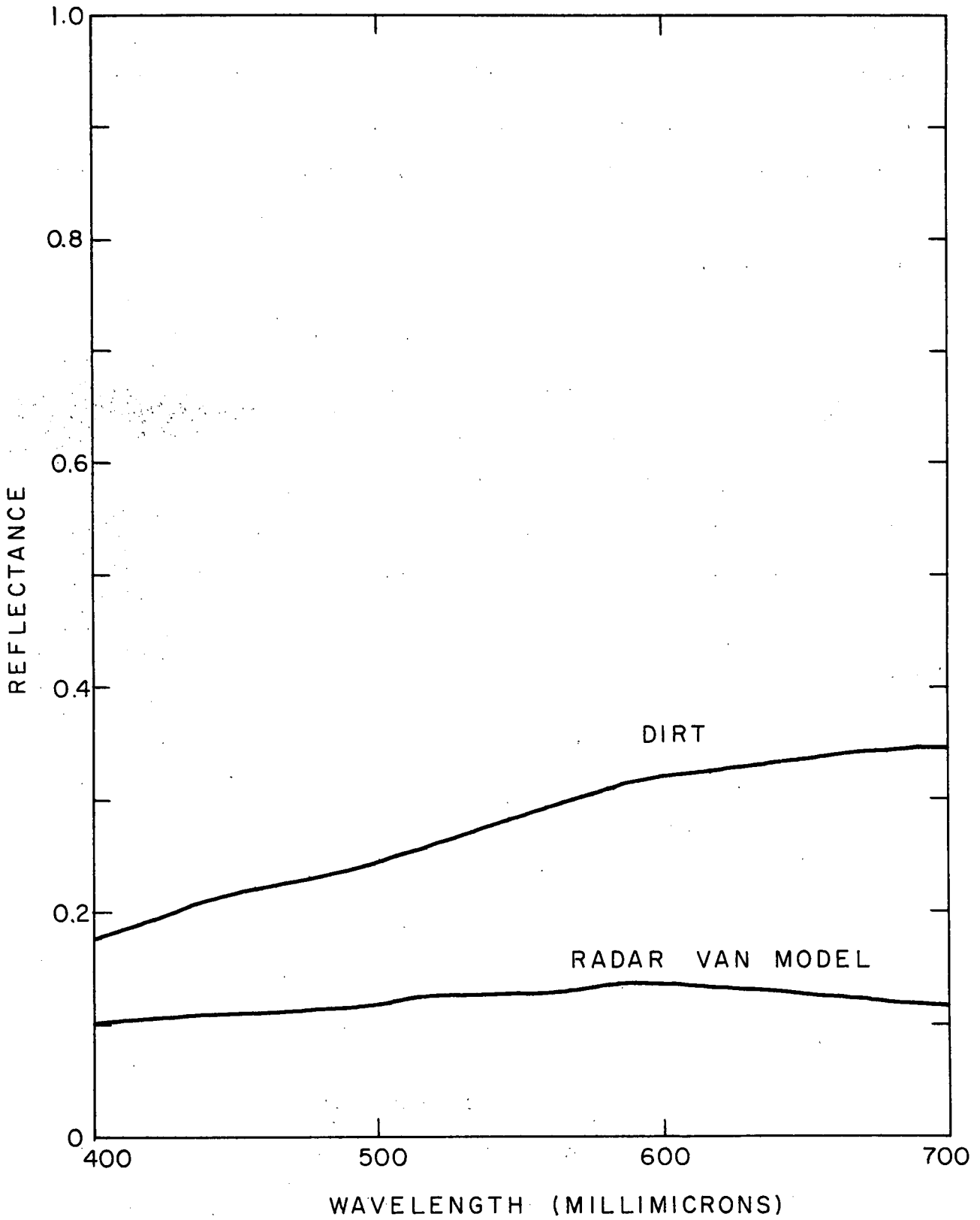


FIGURE 16- SPECTRAL REFLECTANCE OF TARGET AND BACKGROUND

#### 4.2.4 Ground Station.

Photography. The camera on the goniocamera frame was a 35 mm Nikon F. Two lenses were used, having focal lengths of 50 mm and 135 mm. Prior to the experiment a large supply of Plus X film was obtained so that all film used would be from the same lot. Lacking spectral sensitivity on the current Plus X, it was assumed similar to the aerial Plus X and filtered in a similar manner to obtain a photopic response (see Section 4.2.5). The film was developed under rigidly controlled conditions.

The target films were selected to represent the median time for the period of observation at a given altitude. A rough picture of the range of sun positions these median times represented can be obtained from a look at Fig. 17. The points represent all the observations. A separate symbol is used for each target and each observation altitude.

The target films used to make the predictions were densitometered on a special automatic densitometer developed by the RADI Program of the Visibility Laboratory under Bureau of Ships Contract NObs-84075.<sup>5</sup> The output of the densitometer was automatically punched on punch cards. The results of densitometry of the targets and the three grey scales per film strip were thus in a form for use with the Visual Target Classifier Computer Program. (See Section 4.3 for more details on the Computer Programs.)

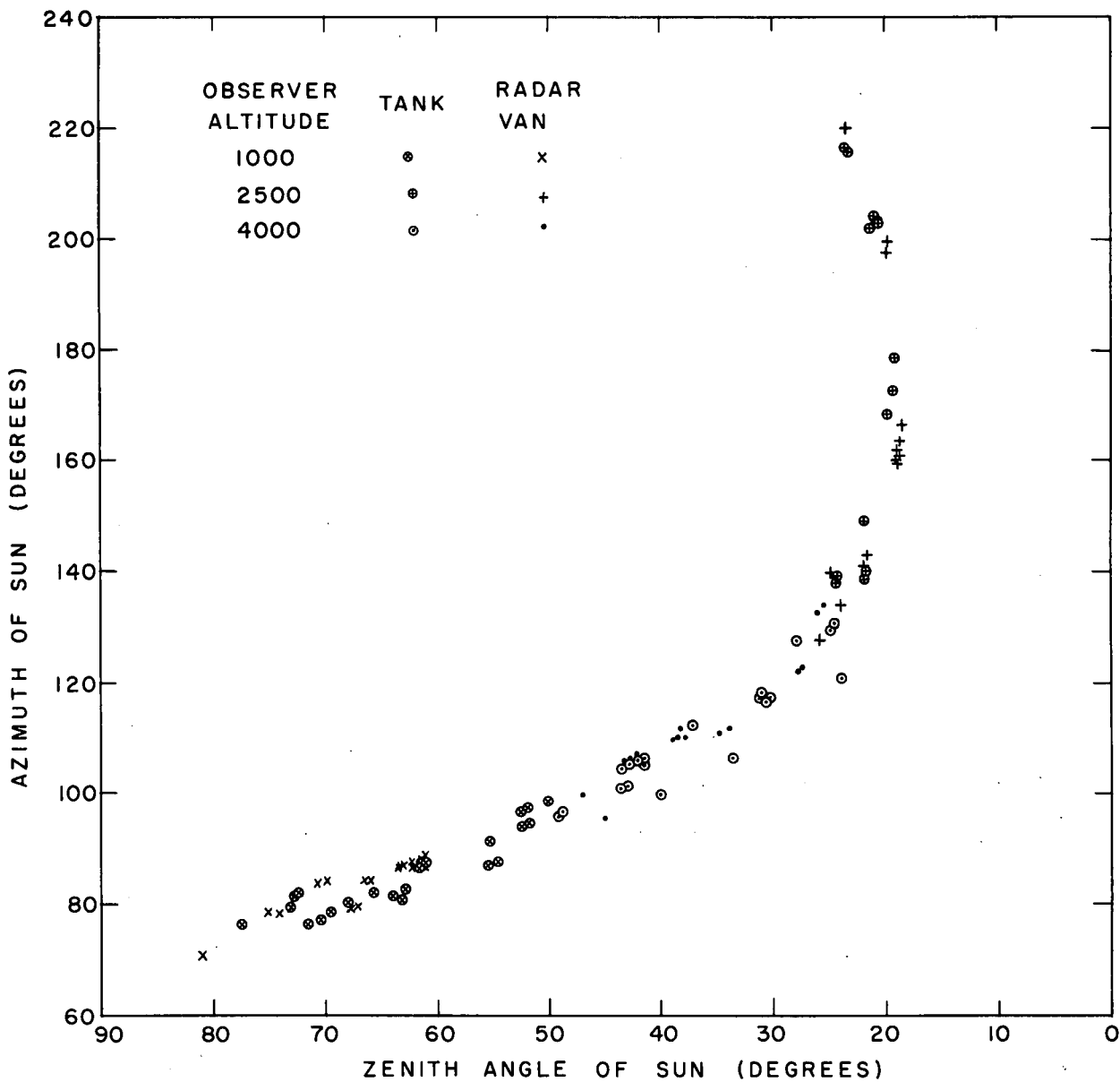


FIGURE 17 - AZIMUTH AND ZENITH ANGLE OF SUN DURING SIGHTINGS



Photometry. The spectral sensitivity of the RCA 931A phototubes in the goniophotometer and illuminometer was measured on the Hardy spectrophotometer. Filters were then selected by means of a careful series of calculations designed to determine the best filter package for obtaining a photopic response. The relative spectral sensitivity of the phototubes with these filters is shown in Figs. 18 and 19. The dotted line is the photopic sensitivity curve.

Both instruments were carefully calibrated both before and after the field trip. A relative calibration was made of the full range of instrument response on an optical bench. An absolute calibration was made on a bar photometer with a 2854° K standard lamp. The change in the calibration of the goniophotometer was less than 7 percent over the three-week period; that of the illuminometer was less than 2 percent; in both cases a mean value was used throughout data reduction.

The illuminometer was fitted with a special diffusing cap which transmitted incident light flux according to the cosine of the angle of incidence. A metal strap in the form of a semicircle rotated azimuthally, alternately shadowing the collector from the sun, and allowing it to be fully sunlit. Thus, with a single instrument both total illumination and shadow intensity could be measured. The measurements of illumination during the sightings are graphed as a function of zenith angle of the sun in Fig. 20. The curve labeled "clear day"

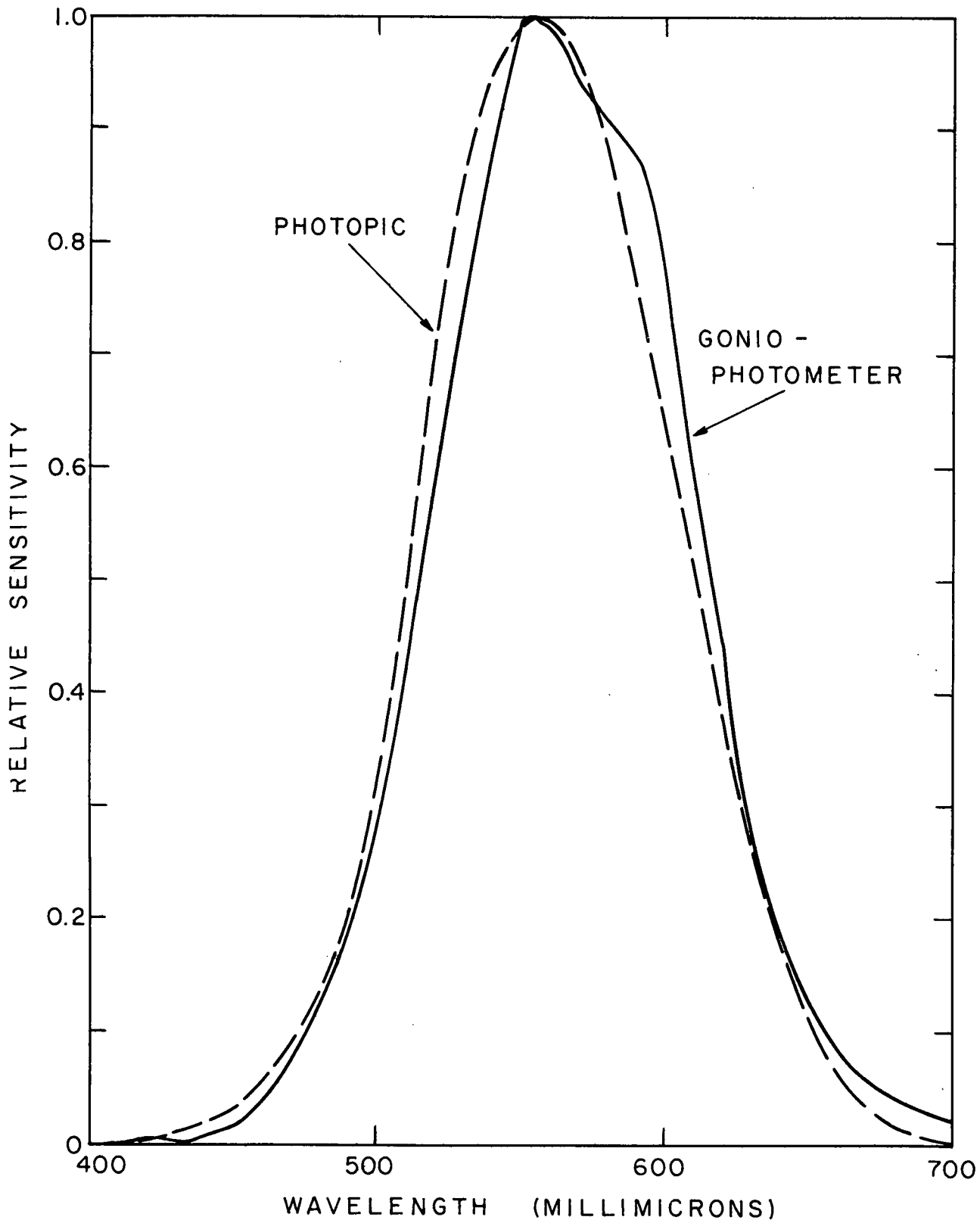


FIGURE 18- RELATIVE SPECTRAL SENSITIVITY OF GONIOPHOTOMETER

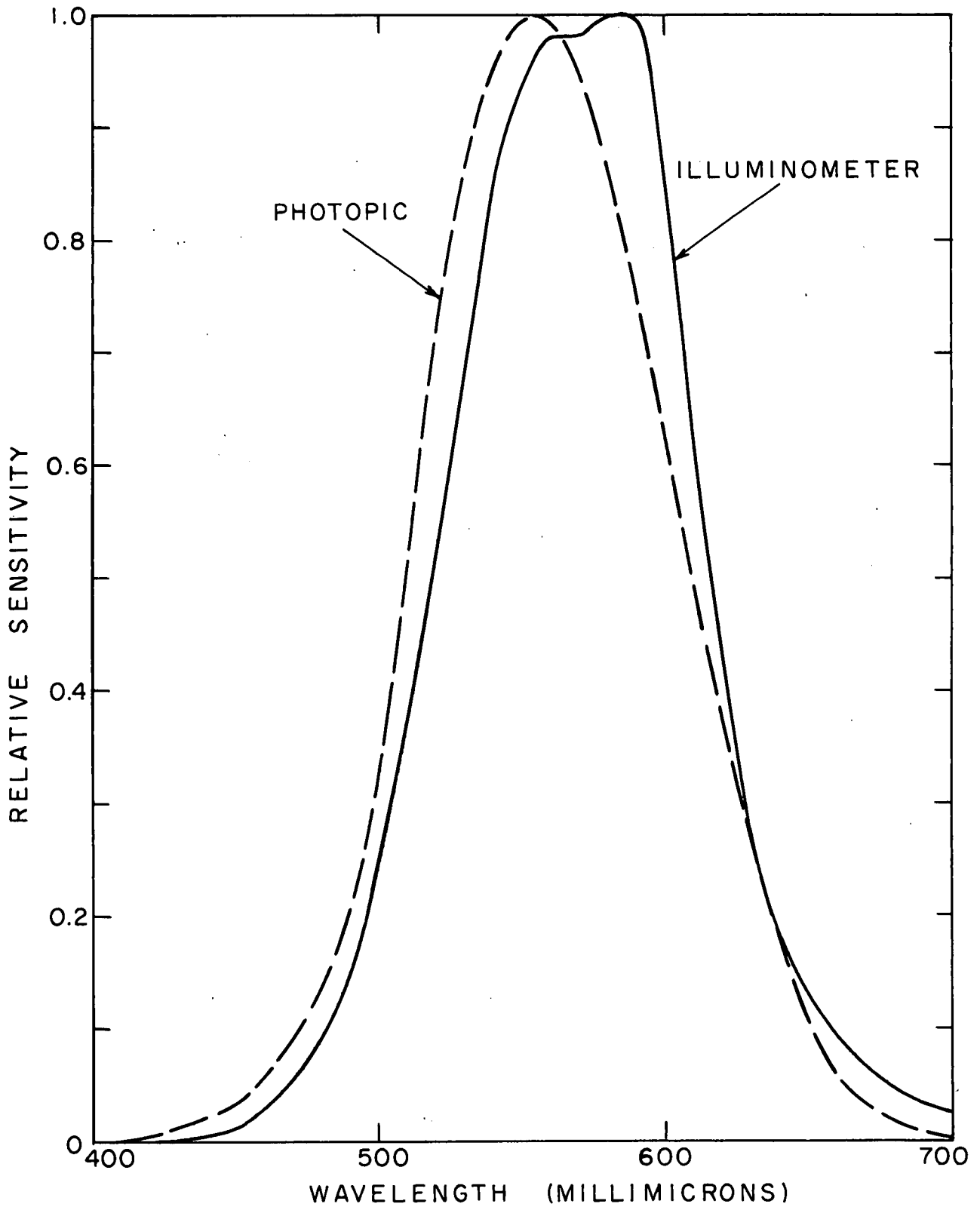


FIGURE 19- RELATIVE SPECTRAL SENSITIVITY OF ILLUMINOMETER AND SHADOW INTENSITY METER

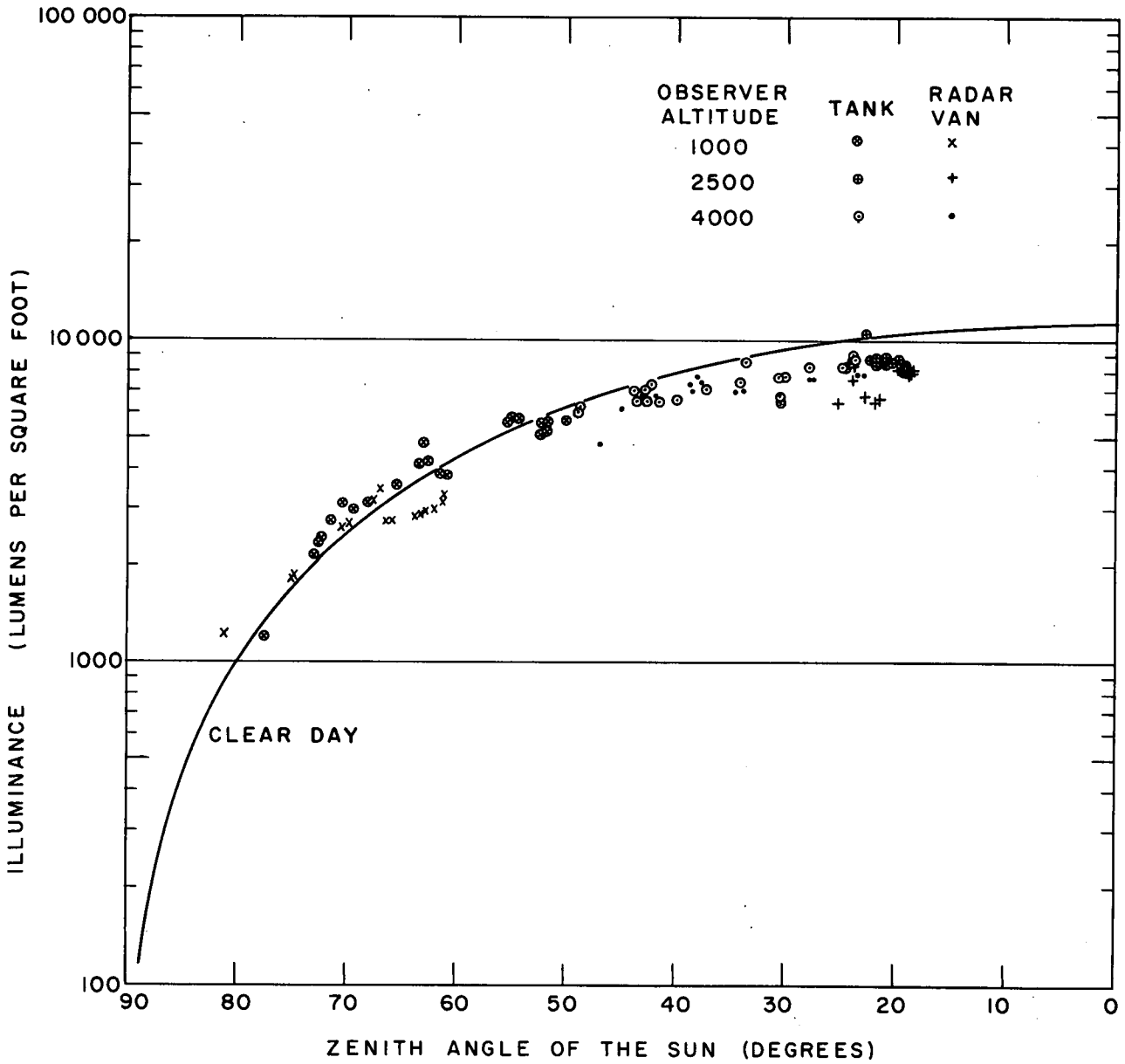


FIGURE 20 - ILLUMINATION DURING SIGHTINGS

is an average clear day based upon a large number of measurements made all over the world.<sup>6</sup> The shadow intensity for each observation is graphed in Fig. 21. The left-hand scale is the ratio of the illumination when the sun is occulted to the total illumination. The right-hand scale is shadow contrast which is equal to the ratio on the left-hand scale minus one. Note that for the clear day conditions of the field experiment shadow intensity shows a greater variability for a given zenith angle of the sun than does the total illumination.

The goniophotometer had a rectangular field of view  $2.8^\circ$  by  $1.9^\circ$ . The smaller dimension was in the direction of the zenith angle of the path of sight. Thus at a photometer position of  $45^\circ$ , the linear area encompassed was nearly square. A sample of the goniophotometer data taken during the observations is given in Fig. 22. Note again that the shadow information shows a greater variability at a given zenith angle of the sun than does the fully illuminated dirt.

4.2.5 Photographic Plane. The camera pod was designed at the Naval Ordnance Test Station. A portion of the blueprint is reproduced in Fig. 23. The forward camera was used for the contrast transmittance measurements. It was a P2 Mauer 220, 70 mm camera with a focal length of 150 mm and a nominal frame rate of 5 frames per second. Prior to the field experiment two cases of 100-foot rolls of aerial Plus X film were set aside for this project so that film with the same emulsion number might be used throughout the experiment.

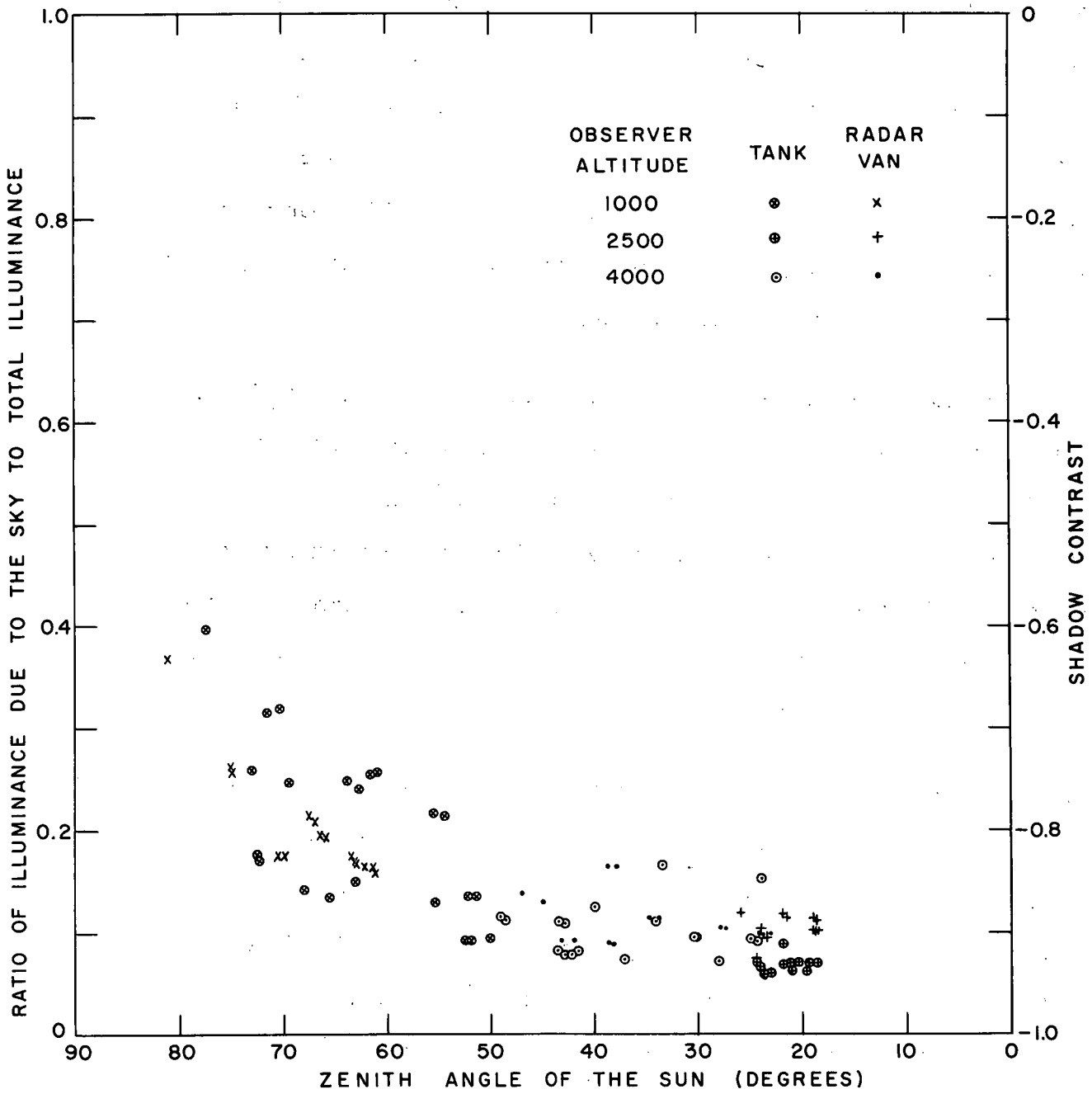


FIGURE 21 - SHADOW INTENSITY DURING SIGHTINGS

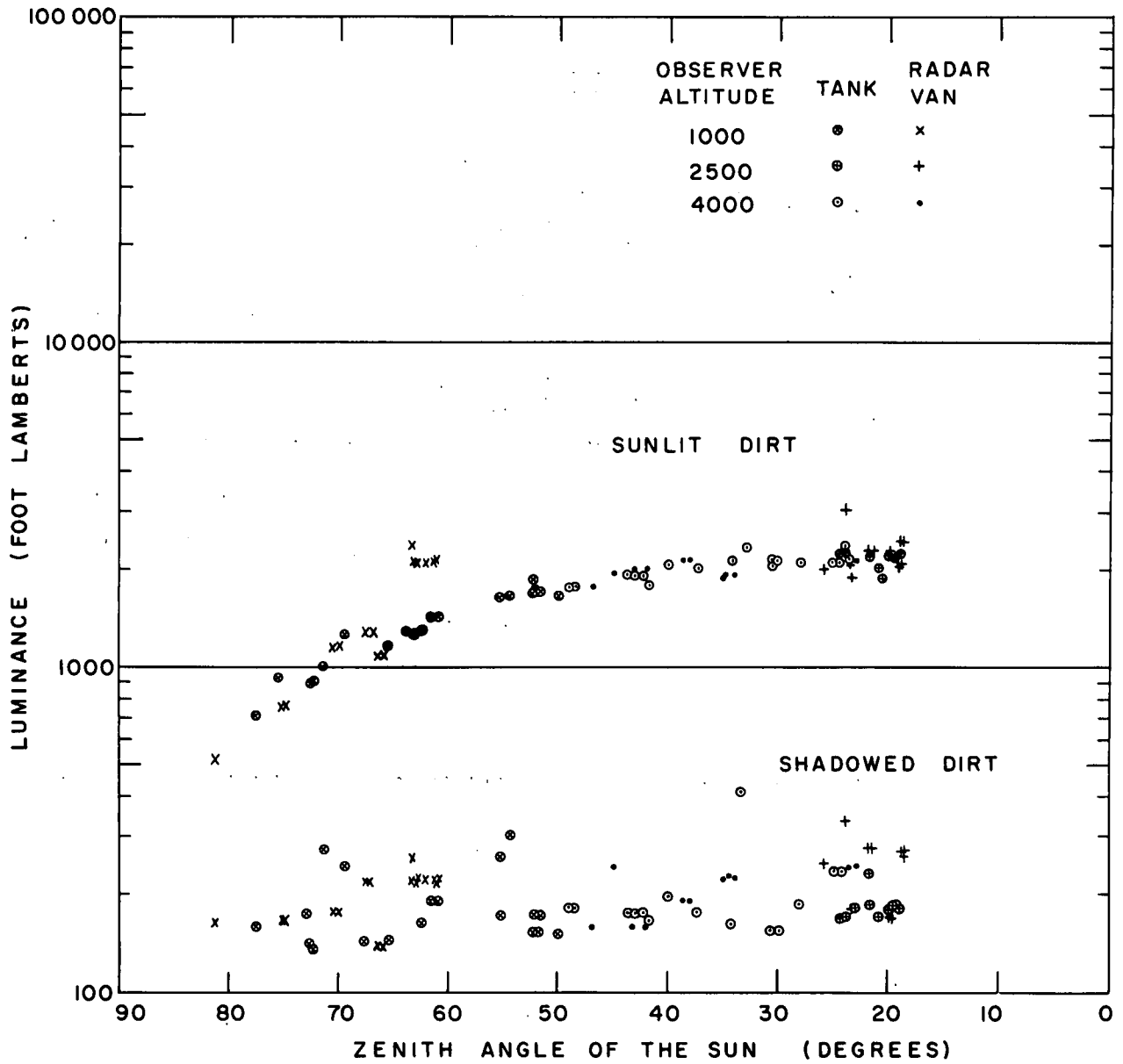


FIGURE 22 - INHERENT LUMINANCE OF BACKGROUND DURING SIGHTINGS  
(PATH OF SIGHT  $10^\circ$  BELOW THE HORIZONTAL)

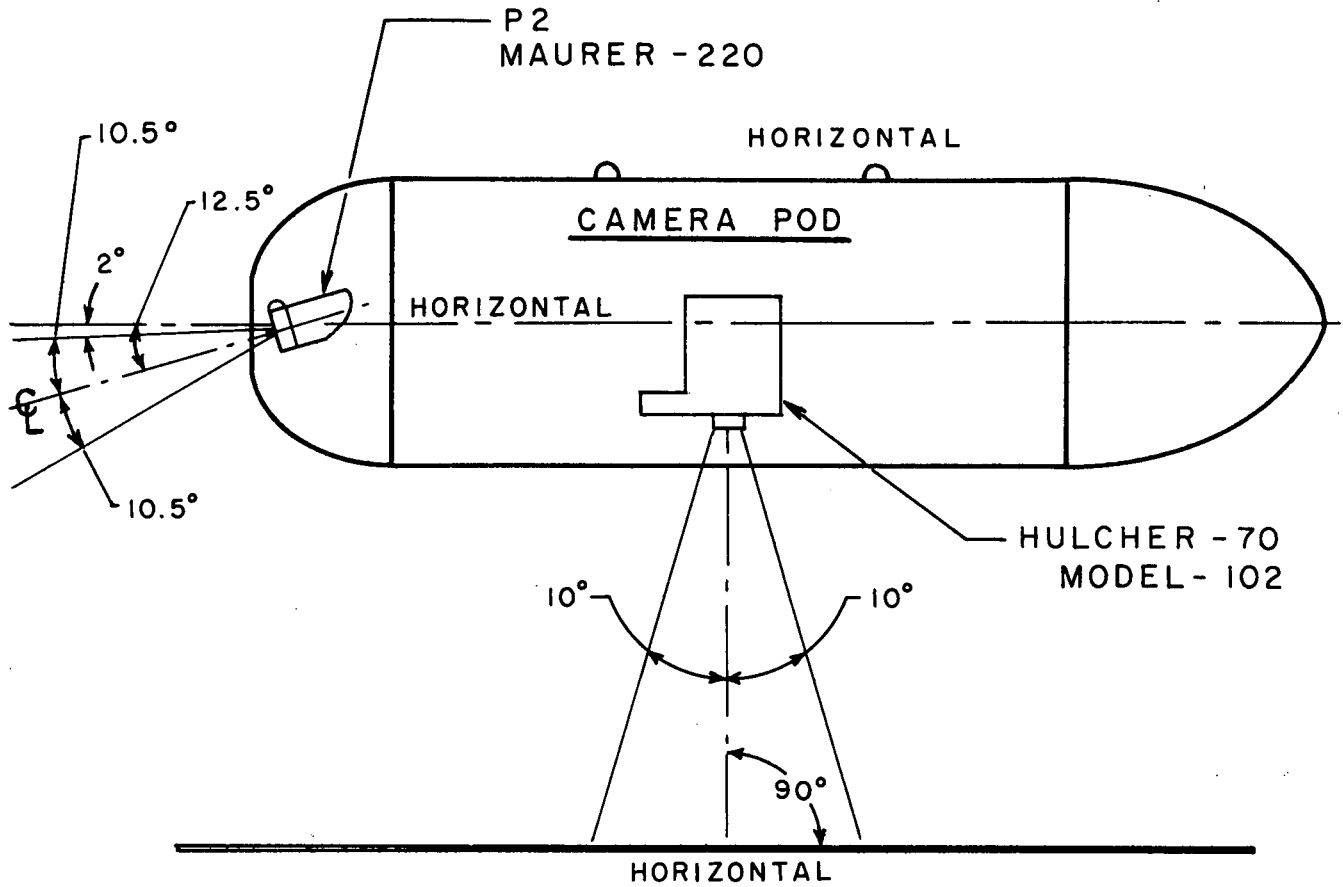


FIGURE 23- DESIGN OF CAMERA POD



The first week a K-2 filter was used on the camera. During the week between the first two weeks of the field test, it was determined that a Wratten 38 filter should be added to the K-2 to obtain a spectral response closer to the photopic response. The relative sensitivity of the Plus X aerial film<sup>7</sup> with the filters is given in Fig. 24.

The contrast loss due to the flat glass window in the camera pod was measured in a similar manner to the contrast transmission measurements of the windscreen of the observation plane (see Section 4.2.6 for method). There was essentially no difference between data taken with or without the glass window.

At the beginning of each photographic flight a picture was taken of a calibrated grey scale held at 50 feet and 100 feet from the airplane on the runway. The film was developed under rigidly controlled conditions by the Visibility Laboratory. First all the grey scales were densitometered and only those flights selected which had data on the straight line portion of the characteristic curve. The gamma for each film was determined by the least squares method.

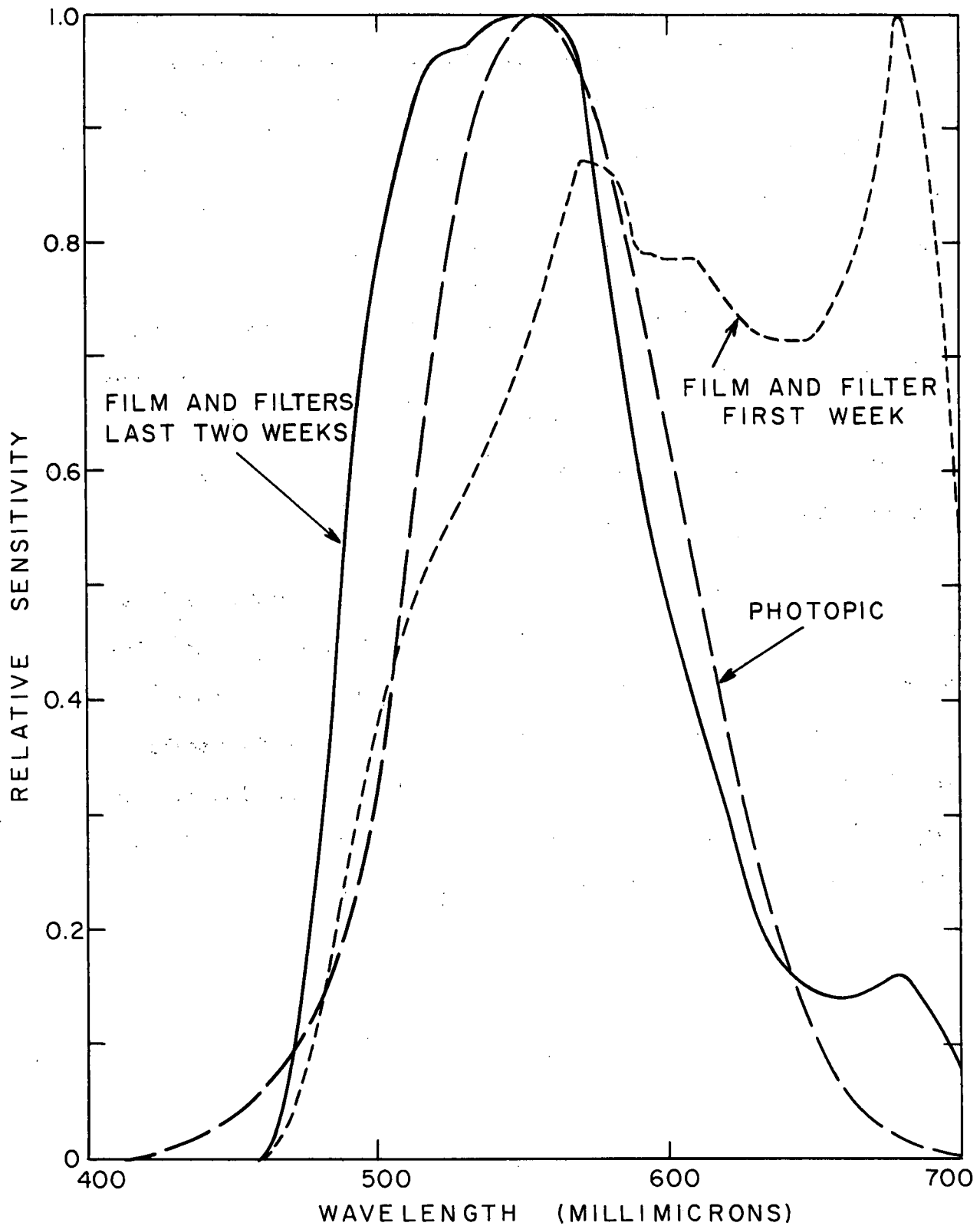


FIGURE 24- RELATIVE SPECTRAL SENSITIVITY OF PLUS-X AERIAL FILM WITH FILTERS

The film densities of the two photographic targets (oil and dirt or sage and dirt) for determining contrast were always measured at closely adjacent points so as to minimize the effect of the uneven exposure across the frame due to the faulty shutter mechanism. Contrast transmittance values were obtained by dividing the contrast of the oil against the dirt from the photograph taken at altitude by the contrast of oil against dirt measured at the ground station with the goniophotometer. Angles of path of sight on the films were determined photogrammetrically from the position of the horizon on the frames. Contrast transmittance measurements using the contrasts of the sage against the dirt were made by dividing the contrast at altitude by the contrast at 100 feet. These data are presented in Fig. 25. The straight line fit to the data takes advantage of the fact that, if the sky-ground ratio does not change with path of sight, the contrast transmittance ( $C_R/C_O$ ) can be reasonably approximated by the following equation:

$$C_R/C_O = \exp \left( - \frac{\bar{R}}{\bar{L}_O} \right)$$

where  $\bar{R}$  is the optical slant range and  $\bar{L}_O$  is an effective attenuation length at ground level.

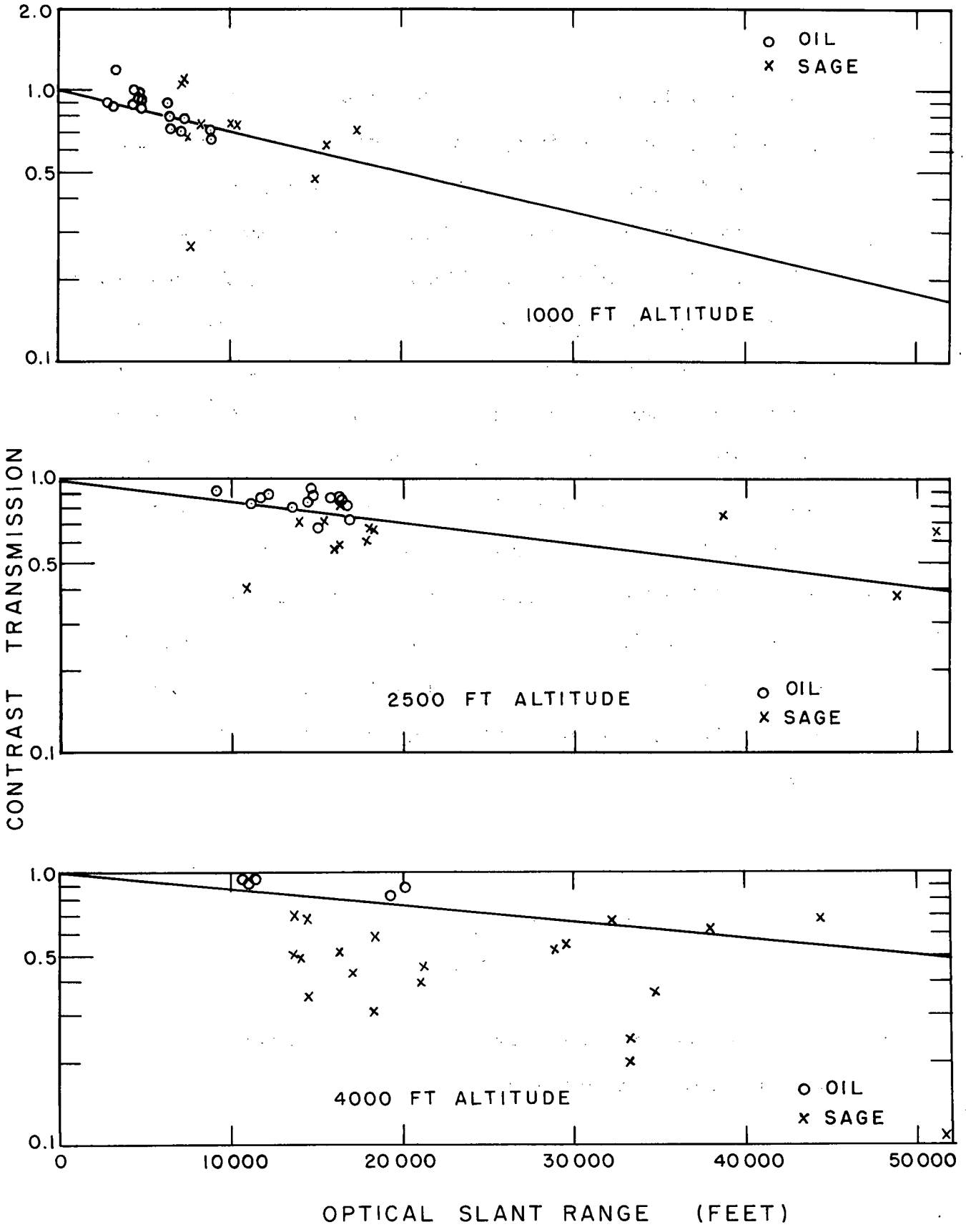


FIGURE 25 - CONTRAST TRANSMISSION OF THE ATMOSPHERE

Since:

$$\ln C_r/C_o = - \frac{\bar{R}}{\bar{L}_o}$$

the slope of the curves in Fig. 25 is negative and equal to  $-1/\bar{L}_o$ . These slopes were found by the least squares method for the 1000 and 2500 ft. altitudes. The scatter in the data at 4000 feet necessitated a different interpretation of these data. It was assumed that the atmosphere from 1000 feet through 2500 feet to 4000 feet contained no optical discontinuities. The slope drawn for the 4000-foot data represents the result of this assumption.

The degree of precision attained by the above approximation can be evaluated by assuming the contrast transmittance at a  $9^\circ$  depression angle of sight to be invariant. The contrast transmittance at other paths of sight then depends upon the assumed sky-ground ratio which is expected to lie between 1 to 2 for desert backgrounds.

The best fit lines on Fig. 25 represent a sky-ground ratio of 1. The difference between different assumptions of sky-ground ratio is seen by examining Table III. The difference was determined to be insignificant at the paths of sight most appropriate for each altitude:  $3^\circ$  at 1000 feet,  $4^\circ$  at 2500 feet, and  $9^\circ$  at 4000 feet.

Table III CONTRAST TRANSMISSION OF THE ATMOSPHERE AS A FUNCTION OF SKY-GROUND RATIO AND DEPRESSION ANGLE OF PATH OF SIGHT

Observer Altitude (Feet)	Sky-Ground Ratio	Contrast Transmittance		
		Depression Angle of Path of Sight		
		3°	9°	19°
1000	1	0.548	0.818	0.908
	1.4	0.560	0.818	0.908
	2	0.572	0.818	0.908
2500	1	0.464	0.774	0.884
	1.4	0.471	0.774	0.880
	2	0.496	0.774	0.877
4000	1	0.397	0.734	0.862
	1.4	0.412	0.734	0.860
	2	0.435	0.734	0.855

#### 4.2.6 Observation Plane

Attitude. The information on attitude of the observing aircraft indicated the following averages for each altitude of observation.

Altitude (Feet)	Attitude (Degrees)	Forward Field of View Below Horizontal (Degrees)
1000	3.9	18.6
2500	5.6	16.9
4000	5.5	17.0

Contrast Transmission of the Windscreen. The photographs of the self-luminous grey scale taken outside the plane established the characteristic curve of the film and a means for converting directly from film density to luminance. Only those frames were used which had the entire grey scale on the straight line portion of the characteristic curve. The characteristic curve was fitted to the data by the least squares method and the densities of the films taken from inside the airplane were converted to luminance values by equation.

The technique for obtaining contrast transmittance is illustrated in Fig. 26. The data are from one of the films taken through the windscreen and reflector.

$bB_o$  = inherent background luminance  
(self-luminous grey scale measured in air)

$bB_r$  = apparent background luminance  
(self-luminous grey scale measured through  
windscreen)

$C_r/C_o$  = contrast transmittance of windscreen

$T$  = beam transmittance of windscreen

$B^*$  = path luminance due to light scattered or  
reflected by windscreen

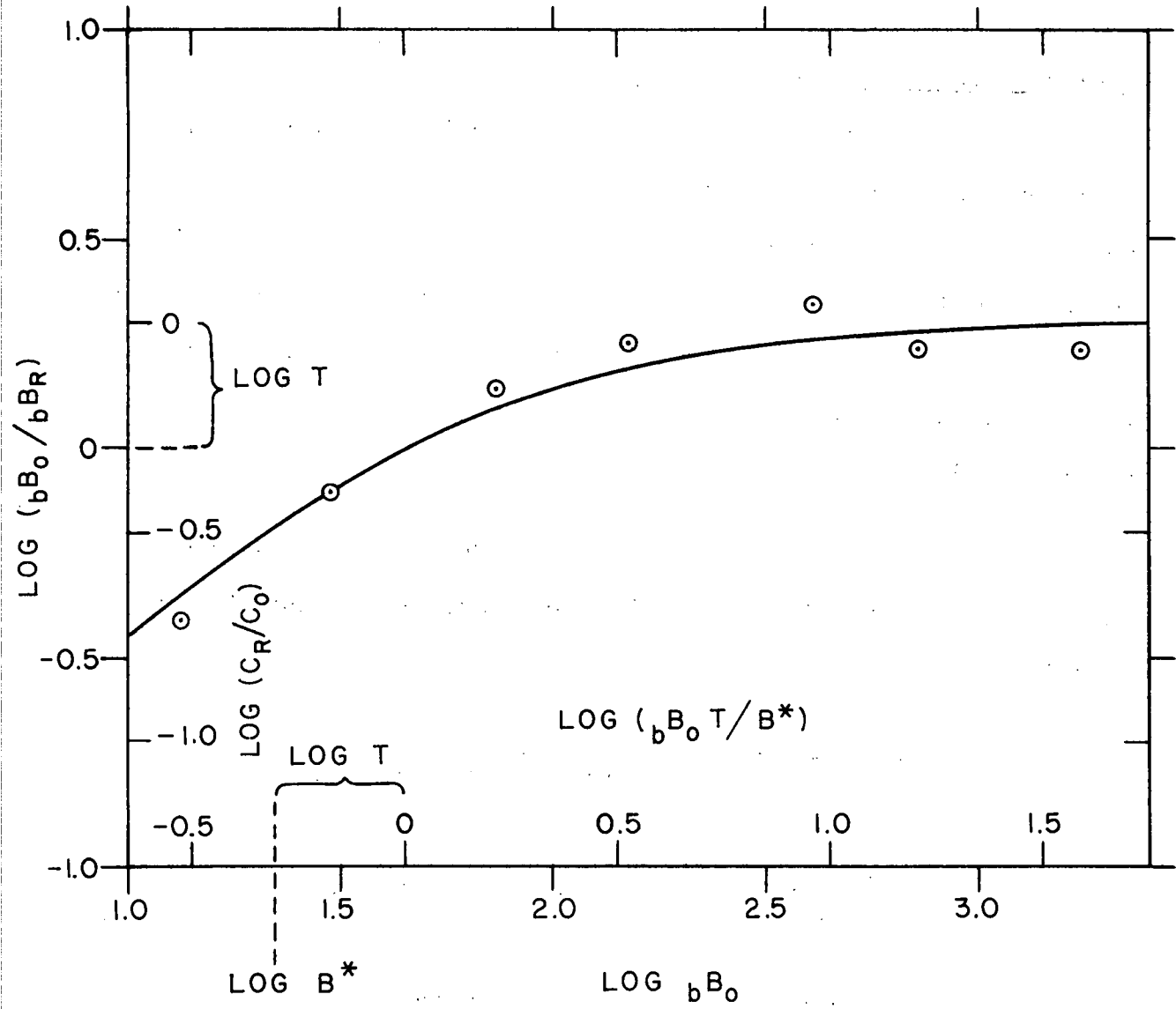


FIGURE 26 - CONTRAST TRANSMISSION OF THE WINDSCREEN



Contrast transmittance is a function of  ${}_bB_0T/B^*$  as follows:

$$\log C_r/C_o = \log \frac{1}{1 + \frac{B^*}{{}_bB_0T}}$$

and as such can be plotted as a function of  ${}_bB_0T/B^*$ . The inner scales go with the solid curve and represent one piece of graph paper.

Contrast transmittance is also a function of  ${}_bB_0/{}_bB_r$ :

$$\log C_r/C_o = \log ({}_bB_0/{}_bB_r) + \log T$$

and

$$\log ({}_bB_0T/B^*) = \log {}_bB_0 + \log (T/B^*)$$

On a similar scale (outside scales on Fig. 26)  $\log ({}_bB_0/{}_bB_r)$  is plotted as a function of  $\log {}_bB_0$ . The vertical and horizontal displacement of the two graphs yields  $\log T$  and  $\log (T/B^*)$  respectively. On the vertical scales:

$$\log T = \log C_r/C_o \text{ when } \log ({}_bB_0/{}_bB_r) = 0.$$

On the horizontal scales:

$$\log B^* = \log {}_bB_0 \text{ when } \log ({}_bB_0T/B^*) = \log T.$$

The contrast transmittance answer is read where the apparent background luminance estimate (the inherent background luminance is expected to be slightly less than the apparent value) is on the  $\log {}_bB_0$  scale. In the instance in Fig. 26, the dirt luminance was 1250 foot-lamberts or greater, therefore the  $\log {}_bB_0 \cong 3.097$  and  $C_r/C_0 \cong 0.97$ .

The average contrast transmittance of the windscreen was 0.96.

4.2.7 Observers. The spectral transmission of the visors on the helmets of the pilots was measured on the Hardy spectrophotometer. These data are presented in Fig. 27. The photopic transmittance of the goggles was calculated to be 0.0401.

#### 4.3 Sighting Range Predictions

4.3.1 Computer Program. The punch cards containing the results of the densitometer measurements of the tank and radar van, and the grey scales for each film strip, were the target data input to the computer programs. There were essentially four parts to the computer program for determining the inherent target index.

1) The information from the three exposures of the grey scale were used to determine one complete characteristic curve for each film strip and this curve was put into analytic form.

2) The densitometer values for each target were converted to relative luminance values by means of the analytic functions determined above. The average background luminance was obtained by averaging the values in the upper left-hand corner of the frame, and the contrast of each part of the target was computed.

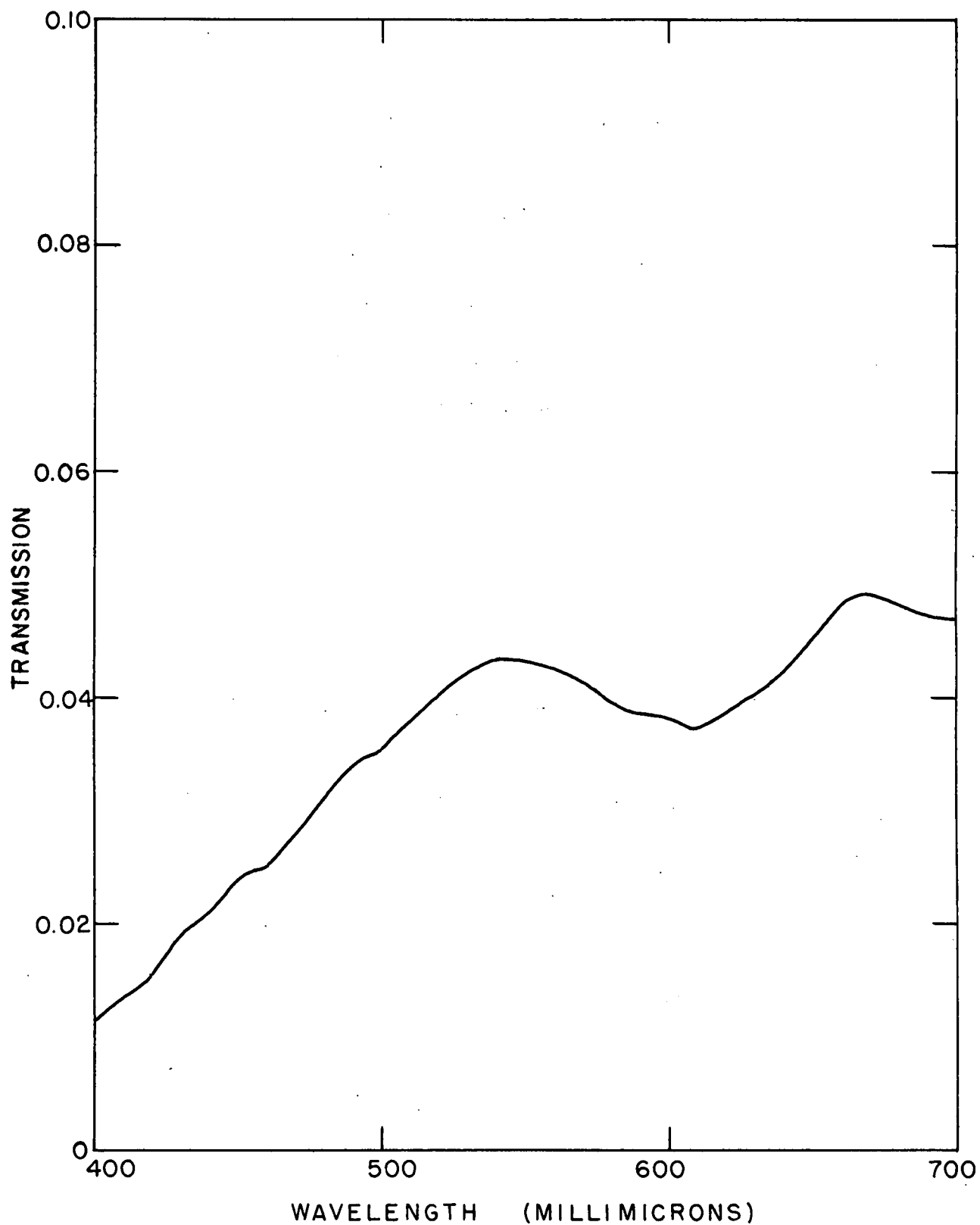


FIGURE 27 - SPECTRAL TRANSMISSION OF THE GOGGLES

3) The densitometry had been accomplished covering a rectangular grid, each element of which was square and small in angular subtense. The third program combined the necessary elements and portions of elements to obtain a grid with elements  $1/2$  by  $1/2$  minutes in angular subtense. This grid was the inherent contrast map of the target. The grid for the radar van at the appropriate angular subtense for an observer at 4000 feet is presented in Table IV.

Table IV INHERENT CONTRAST MAP OF RADAR VAN

Row	Column	1	2	3	4	5	6	7	8
1		+0.049	+0.001	+0.005	-0.016	-0.410	-0.471	-0.129	+0.006
2		+0.011	-0.038	-0.037	-0.055	-0.762	-0.848	-0.320	+0.004
3		-0.014	-0.087	-0.217	-0.278	-0.806	-0.811	-0.348	-0.027
4		-0.059	-0.276	-0.764	-0.763	-0.699	-0.635	-0.254	-0.023
5		-0.031	-0.069	-0.073	-0.064	-0.062	-0.074	-0.066	-0.036

Observer altitude: 4000 Feet  
Depression Angle of path of sight:  $9^{\circ}$

4) The final program performed the convolution integral of the target contrast and the summative function for the appropriate visual data. The result was the inherent target index appropriate to the target as seen by the observer at a given altitude and path of sight.

A comparison was made between target indexes derived from the summative function program and those determined by graphical methods. The target chosen was a simple one visually and the comparison is excellent as can be seen in Table V. The two methods would expect to yield results further apart for the early morning targets with the long shadows and odd overall shapes. A target containing both positive and negative elements would compare least well, with the summative function representing the visual response more accurately than the graphical method.

Table V      COMPARISON OF INHERENT TARGET INDEXES DERIVED FROM  
SUMMATIVE FUNCTIONS WITH THOSE DETERMINED GRAPHICALLY

Angle from Fixation	INHERENT TARGET INDEX	
	Summative Function	Graphical
0	24.1	23.4
1.25	17.3	17.2
2.5	12.0	11.3
5.0	6.73	6.53
7.5	4.78	4.84
10.0	3.61	3.78
12.5	2.92	2.93

Target: Radar Van    Observer Altitude: 4000 Feet  
Depression angle of path of sight: 9°

4.3.2 Calculation of Sighting Range. The inherent target index is multiplied by the contrast transmittance of the atmosphere and the contrast transmittance of the windscreen to obtain the apparent target index. All the indexes for one target at one altitude are then graphed as a function of depression angle of the path of sight as in Fig. 28. This graph is used to interpolate to find the appropriate depression angle for each angle from fixation for an assumed field factor. The dotted line represents the field factor 3.6. These interpolated depression angles are next graphed as a function of the angle from fixation as illustrated in Fig. 29. The definition of the boundaries of the detection lobe is determined using this graph. The center of the lobe is the depression angle of the path of sight. The depression angle of the forward edge of the lobe is found at the intersection of a  $45^\circ$  line from the path of sight scale to the solid curve. This is the point where the angle from fixation is equal to the difference between the paths of sight representing the forward edge and the center. The depression angle of the reverse edge is found in a similar manner.

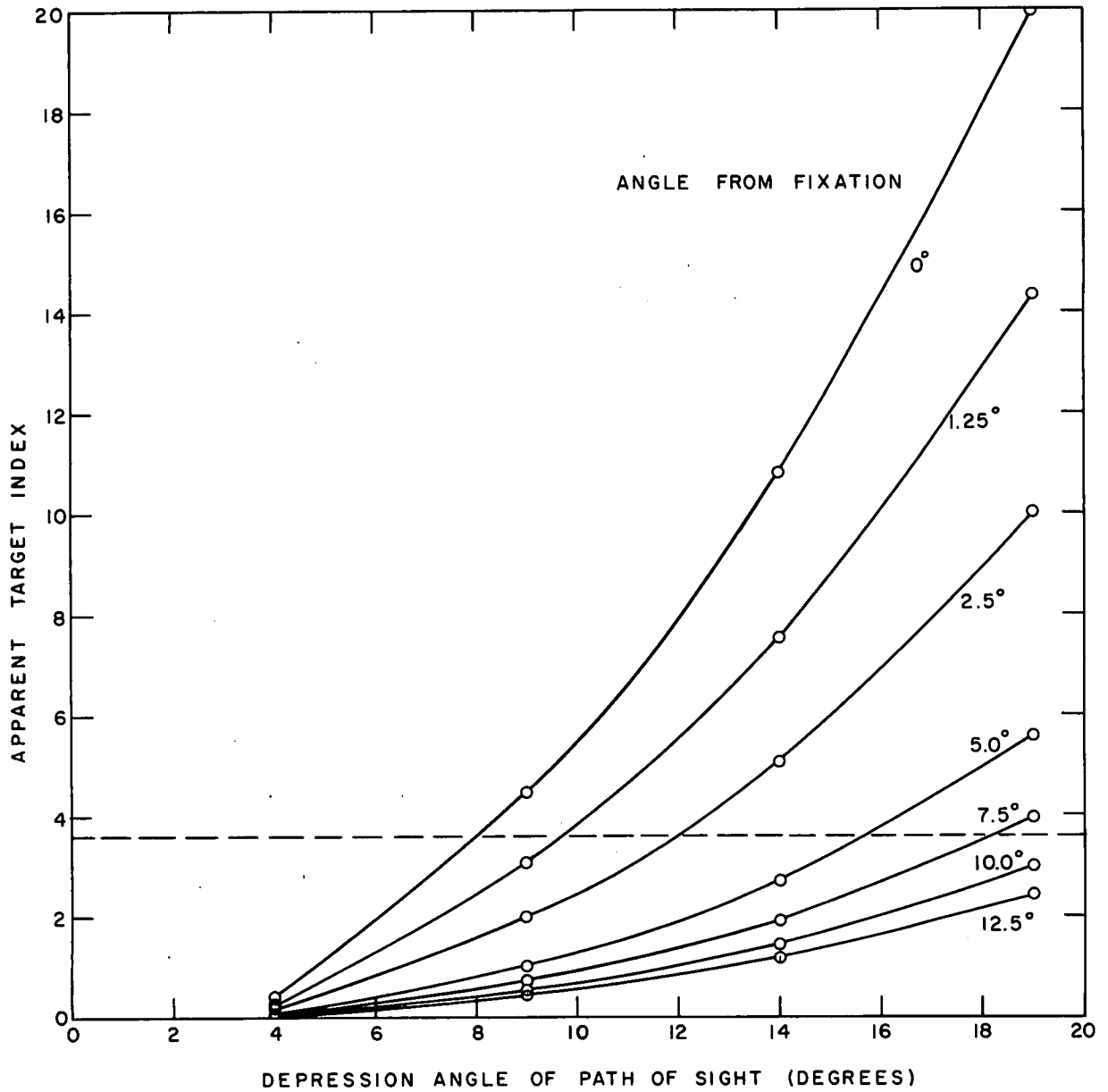


FIGURE 28 - PREDICTIONS OF VISUAL RESPONSE TO THE RADAR VAN FOR THE OBSERVER AT AN ALTITUDE OF 4000 FEET

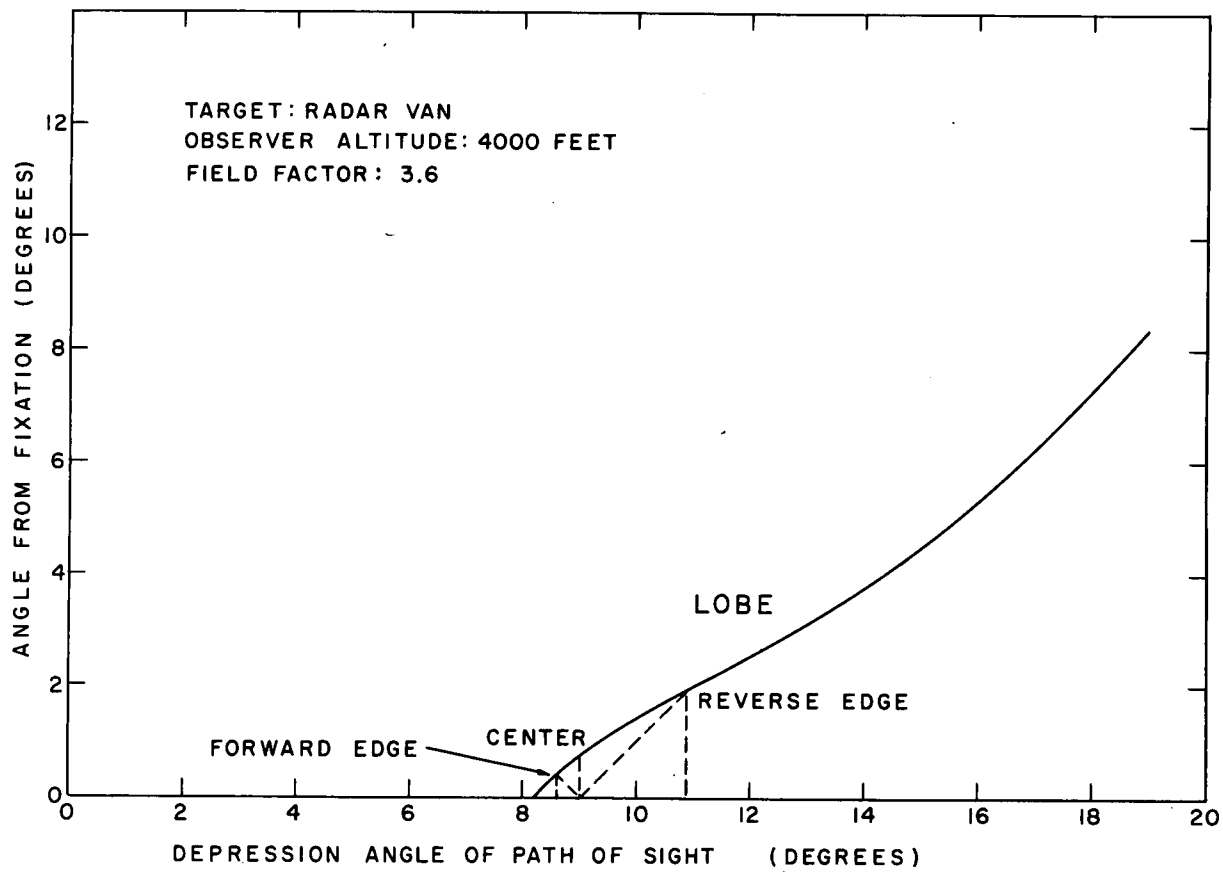


FIGURE 29 - ANGULAR DEFINITION OF THE DETECTION LOBE



These depression angles defining the lobe are determined for a series of paths of sight for the center of the lobe. The depression angle data are then converted to the appropriate horizontal distance from the observer for the altitude of observation. On a linear scale the horizontal distances for the center and edges of the lobe are graphed as a function of the horizontal distance to the center of the lobe, as in Fig. 30. The horizontal line near the top of the graph illustrates one linear definition of the detection lobe for one path of sight.

Three curves are drawn connecting all the forward edge points, center points, and reverse edge points. This graph may now be interpreted in the manner illustrated by the vertical dotted line at the lower edge of the graph. A vertical line drawn through the three solid curves defines the linear limits of the paths of sight in which detection can occur for the observer-to-target distance of 17 500 feet.

The probability for one look ( $P_i$ ) at a given observer-to-target distance is defined by the distance increment (above) representing the paths of sight in which detection can occur ( $\Delta D$ ) divided by the region within which the observer will search ( $R$ ).

$$P_i = \frac{\Delta D}{R}$$

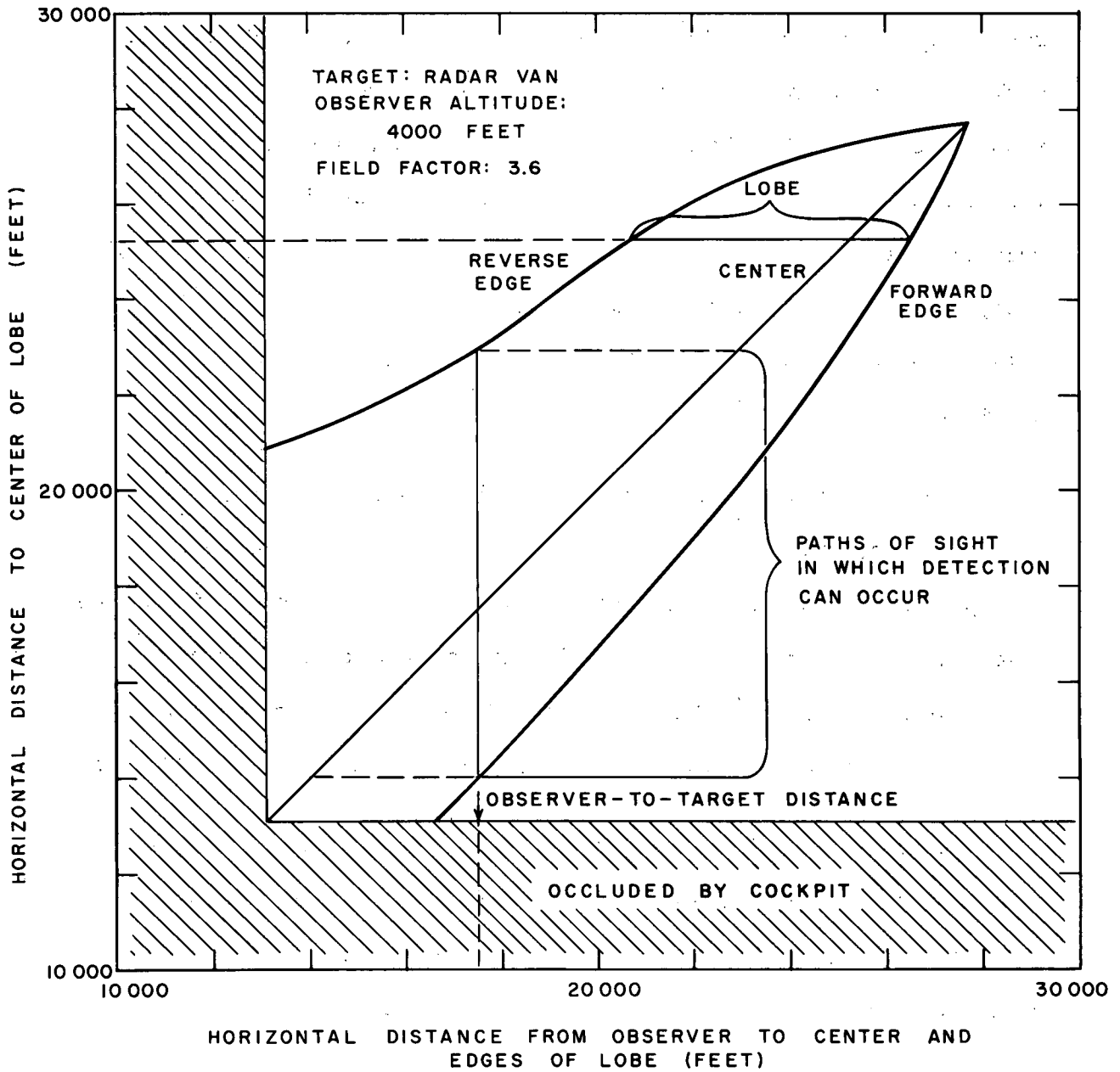


FIGURE 30 - LINEAR DEFINITION OF THE DETECTION LOBE, AND THE PATHS OF SIGHT APPROPRIATE TO DETECTION AT A GIVEN OBSERVER-TO-TARGET DISTANCE

This search region will be defined next. The angular picture of the forward field of view as a function of flight time after passing the 40 000 South point on the bulldozed strip, is depicted in Fig. 31. All of the region within which the target is expected to appear, 0 North to 26 000 North, is visible forward at the 4000-foot observation altitude until 65 seconds have elapsed. However, for the first 28 seconds the radar van is too small to be detectable anywhere in the target region.

A linear representation of this same forward field of view is depicted in Fig. 32. For a random search case, the search region is 26 000 feet (the vertical distance between the two solid lines) until 65 seconds flight time. From then on the region is defined by the vertical distance in the unshaded region between cockpit edge and the 26 000 North position.

It was assumed that the pilot would probably have a rough idea of how far he could see the target and would therefore restrict the region in which he would search to a distance somewhat above the foveal threshold distance. The parallelogram bounded by a line 2000 feet beyond foveal distance, the cockpit, and 0 and 26 000 North, defined the search region at each flight time for the systematic search.

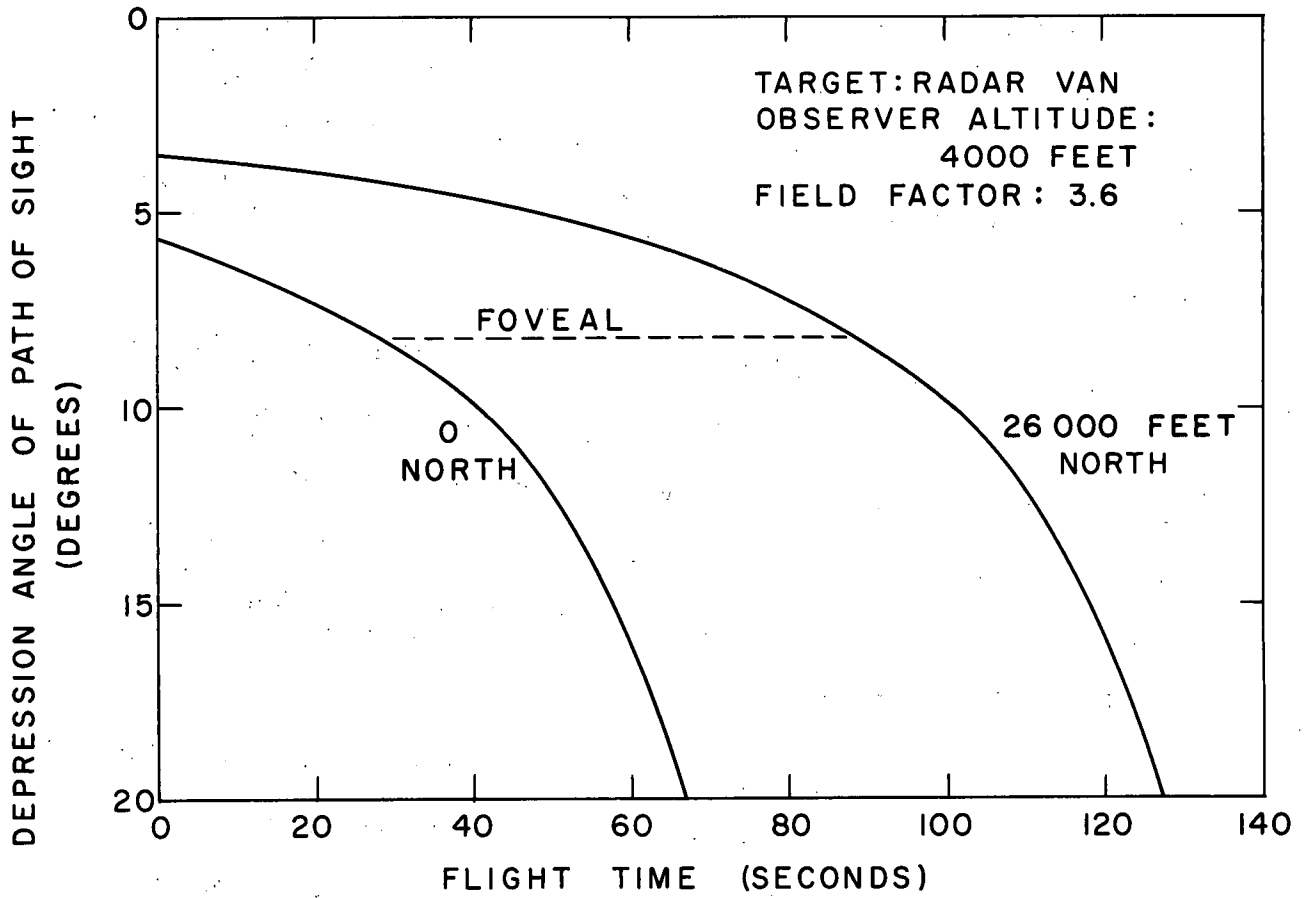


FIGURE 31 - ANGULAR SUBTENSE OF BULLDOZED STRIP AND ITS POSITION IN THE FIELD OF VIEW AS A FUNCTION OF FLIGHT TIME

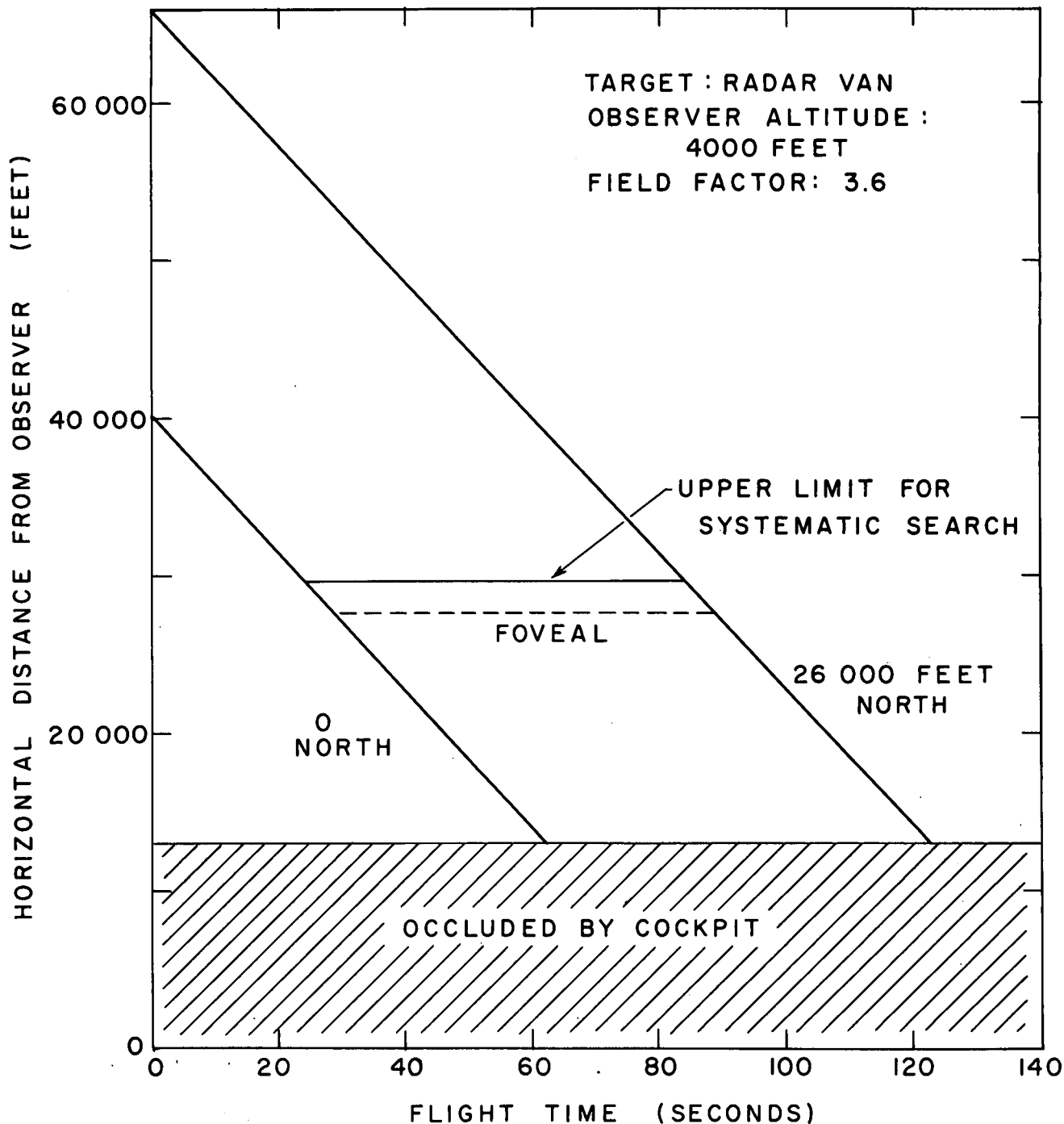


FIGURE 32-LINEAR REPRESENTATION OF THE FIELD OF VIEW AS A FUNCTION OF FLIGHT TIME

The probability of detection for one look for systematic search was graphed as a function of observer-to-target distance for each target position used in the field experiment. This is illustrated in Fig. 33. The 0 and 26 000 North positions were not used in the experiment but they are included on the graph to illustrate the range of the probabilities as a function of target position on the bulldozed strip.

The cumulative probability ( $P_c$ ) for systematic search, in which it is assumed there will be some redundancy in the search pattern is defined as follows:<sup>8</sup>

$$P_c = 1 - \prod (1 - P_i) .$$

The cumulative probability of detection is graphed as a function of horizontal distance from observer-to-target for each target position in Fig. 34.

The relationship of the median and the mean (or average) to the cumulative probability curve is illustrated in Fig. 35. The median is the distance at the cumulative probability of 50 percent. The normal distribution bargraph is recovered from the cumulative probability by taking the differential of the integral. The mean is found by summing the product of the distance times the weighting as assigned by the bargraph. The median and average (or mean) sighting distances reported in Section 3.2 are the values for each target position weighted by the number of observers at each target position, divided by the number of observers for the given target at that altitude of observation.

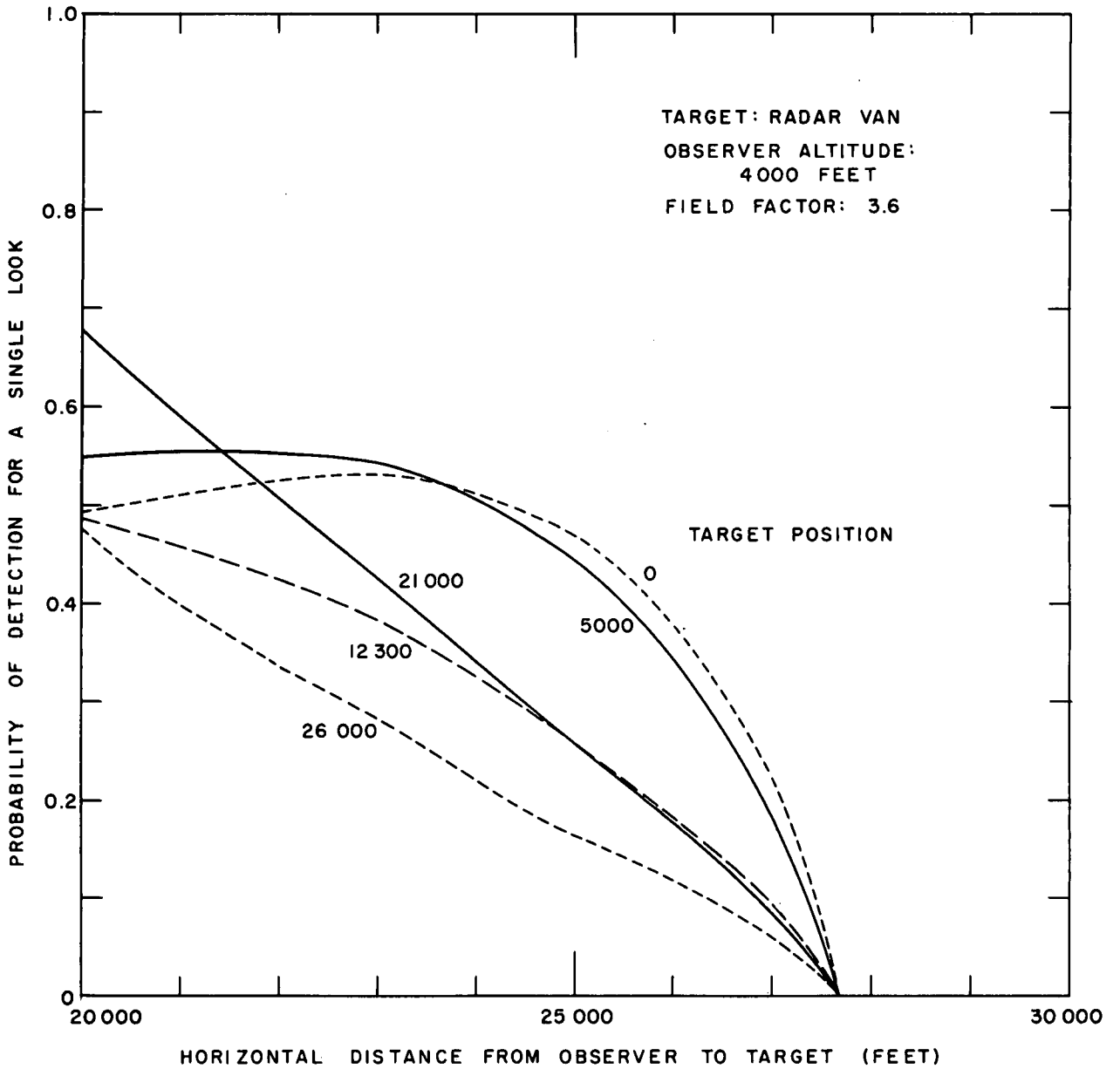


FIGURE 33 - PROBABILITIES FOR ONE LOOK FOR SYSTEMATIC SEARCH AS A FUNCTION OF OBSERVER-TO-TARGET DISTANCE AND TARGET POSITION

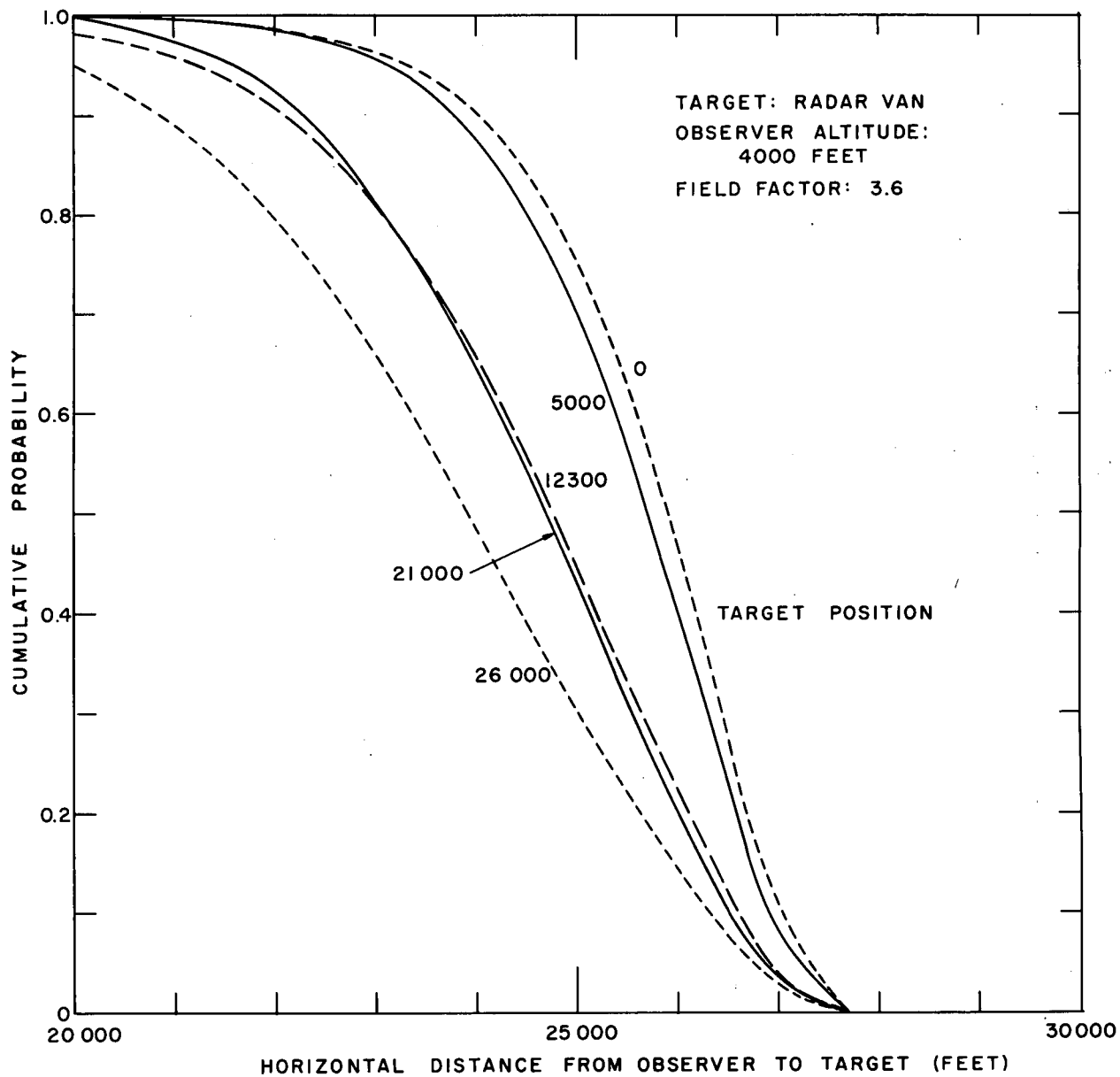


FIGURE 34 - CUMULATIVE PROBABILITY OF DETECTION FOR SYSTEMATIC SEARCH



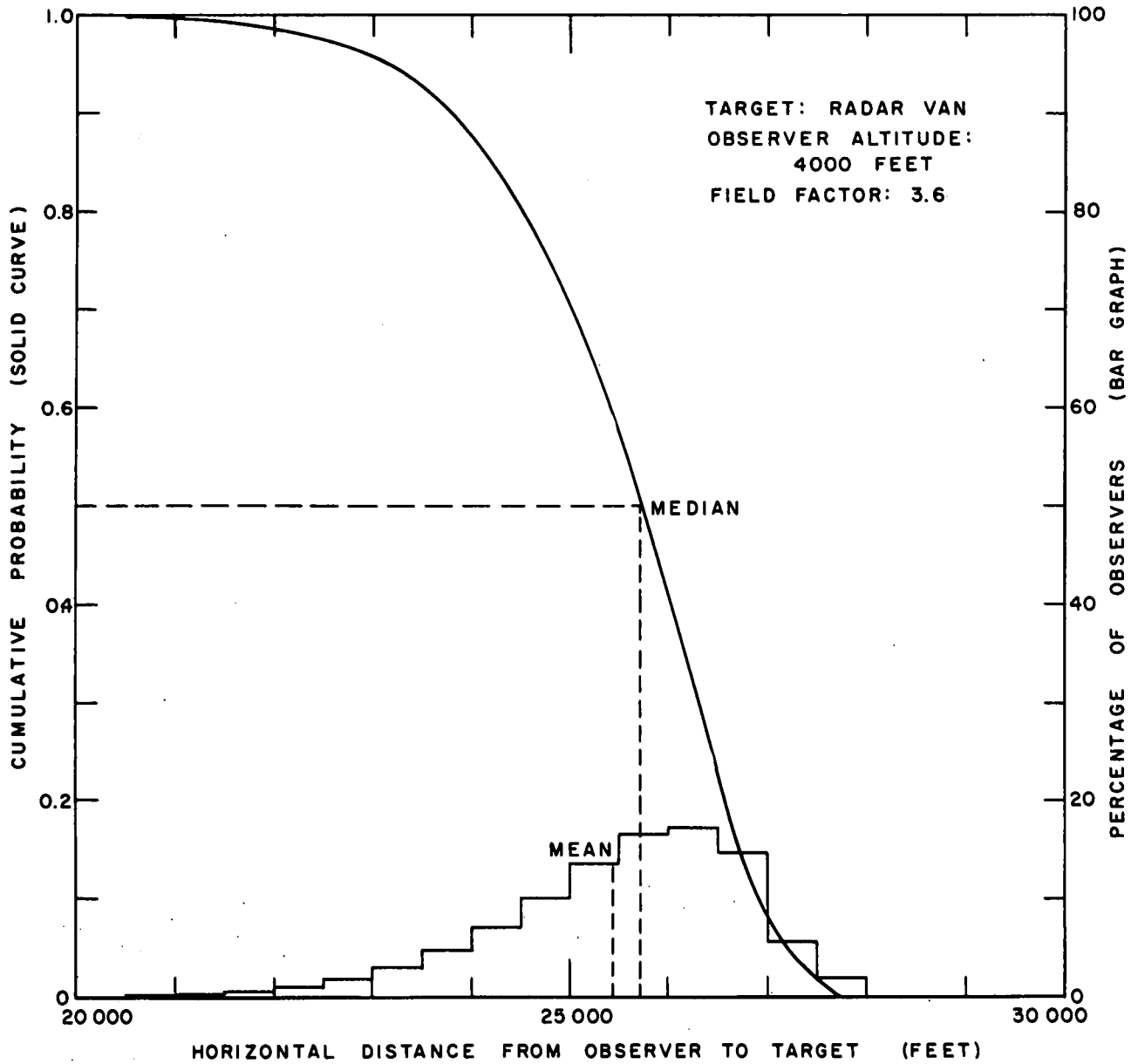


FIGURE 35 - THE PREDICTED MEAN AND THE MEDIAN SIGHTING DISTANCES FOR TARGET POSITION 5000 NORTH

#### 4.4 Predictions of Recognition

4.4.1 Computer Program. The recognition computer program was essentially in four separate parts.

1) The angular subtense of the original contrast grid for the radar van and the tank was examined for each altitude of observation and path of sight. The target with the grid elements having the smallest size was made equivalent to the larger grid element size for each path of sight by the appropriate combination of grid elements. This is similar to step (3) in the detection program.

2) The grids for the radar van and the tank of equivalent grid element size, at each path of sight were superimposed one on top of the other. A sum of the products of the two contrasts was computed for all possible superpositions. The superposition yielding the maximum sum of the products designated the position of greatest equivalency. In this superposition the contrast of the tank was subtracted from the contrast of the radar van.

3) The contrast difference grid, which still had elements very small in angular subtense, was converted to a grid having elements  $1/2$  minute in angular subtense. (This is the same step as (3) in the detection program.) This grid served as the contrast difference map for use with the visual thresholds. An example of one of these maps is given on Table VI.

Table VI MAP OF INHERENT CONTRAST DIFFERENCE BETWEEN THE RADAR VAN  
AND THE TANK

Row	Column	1	2	3	4	5	6	7	8
1		+0.048	-0.037	-0.048	-0.055	-0.415	-0.492	-0.142	-0.010
2		+0.011	-0.043	-0.016	-0.027	-0.233	-0.422	-0.297	+0.017
3		-0.015	-0.096	-0.186	-0.065	-0.088	-0.235	-0.134	-0.015
4		-0.058	-0.263	-0.619	-0.163	-0.115	-0.081	-0.053	-0.023
5		-0.031	-0.082	-0.039	-0.029	-0.028	-0.042	-0.051	-0.032

Target Altitude: 4000 Feet

Depression angle of path of sight:  $9^{\circ}$

4) The signal difference map was the target information for the convolution integral. The visual thresholds from which the appropriate visual summative function had been derived for use in the recognition program were for long fixation times for a background luminance of 100 foot-lamberts.<sup>9</sup> The convolution integral of the visual summative function and the contrast difference was computed resulting in the inherent target index for the signal difference.

4.4.2 Recognition Calculations. The inherent target index for the signal difference was multiplied by the contrast transmittance of the atmosphere and the contrast transmittance of the windscreen to obtain the apparent target index.

The cumulative probability for conditional recognition was defined as the cumulative probability that the signal difference could be detected if the target itself had already been detected with 100 percent probability of detection 2.7 seconds earlier. The 2.7 second time interval was to allow the observer to fixate on the target long enough to maximize his contrast sensitivity and to allow for cortical functioning.<sup>10</sup>

The relationship of the cumulative probability of conditional recognition to the target index for the signal difference was assumed to be similar to the relationship defined by an earlier psychophysical experiment on signal differences.<sup>11</sup> Figure 36 contains a graph of that relationship.

The computer program and the contrast transmittance information provided the measure of apparent target index as a function of depression angle of path of sight for each observer altitude. By means of the graph in Fig. 36 this was translated into a graph of cumulative probability as a function of depression angle of path of sight.

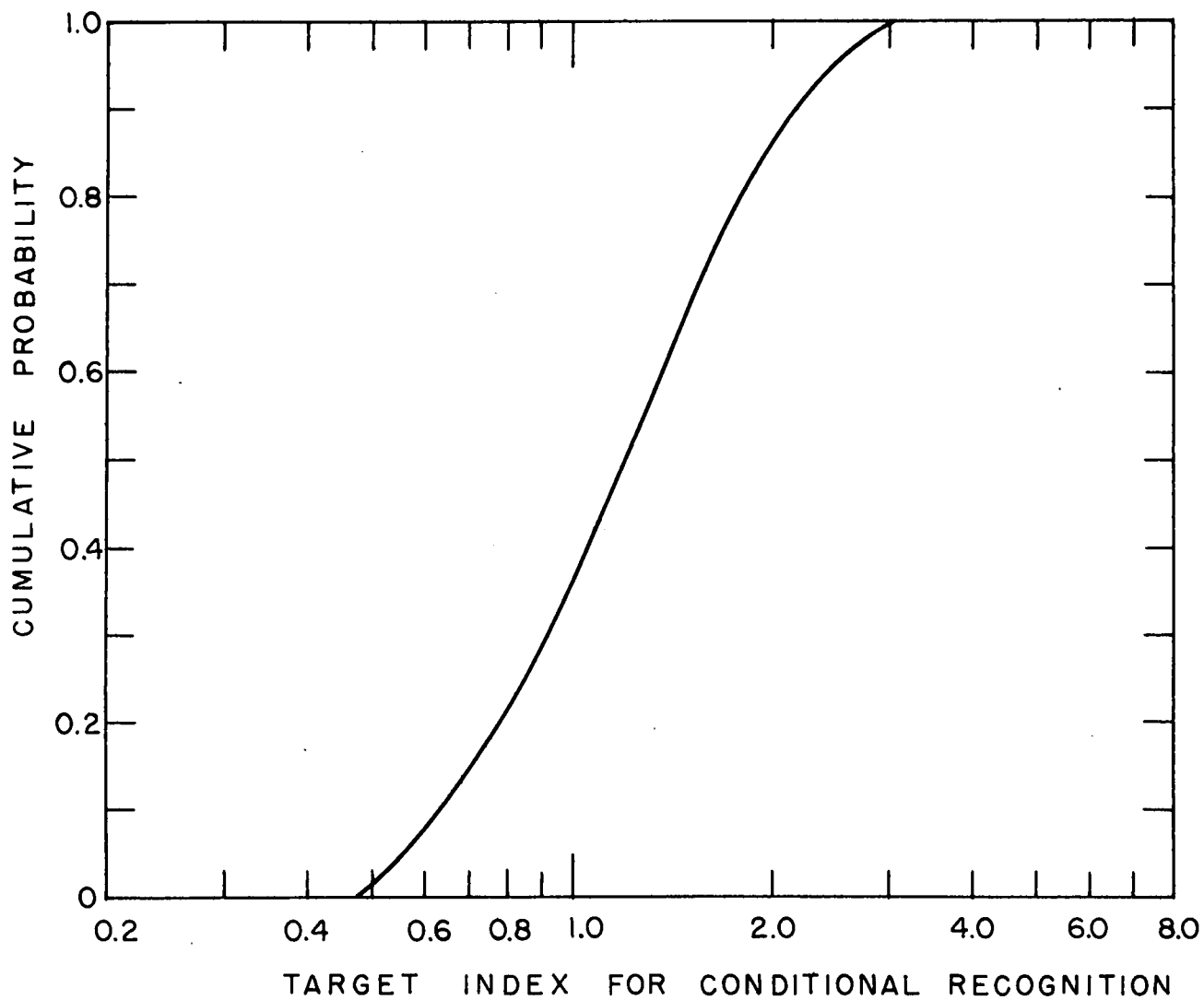


FIGURE 36 - CUMULATIVE PROBABILITY OF RECOGNITION  
IF TARGET HAS BEEN DETECTED WITH 100%  
PROBABILITY FOR 2.7 SECONDS OR MORE.

Finally the horizontal distance from the observer to target was computed from the depression angles. Then a graph of cumulative probability for conditional recognition as a function of horizontal distance was made as in Fig. 37. The cumulative probability of detection for field factor 3.6 for the radar van from the observer altitude of 4000 feet is the middle curve. The innermost curve is the probability of detection applied to distances representing 2.7 seconds after detection.

The final probability of recognition at each observer-to-target distance is the product of the probability of conditional recognition and the probability of detection applied to 2.7 seconds after detection. In all cases related to this field experiment, the probability of conditional recognition had reached 100 percent before the probability of detection applied to 2.7 seconds after detection had become greater than zero. Therefore, it was predicted as an upper limit that the recognition could occur 2.7 seconds after detection, or at a distance 1200 feet closer than the appropriate detection distances.

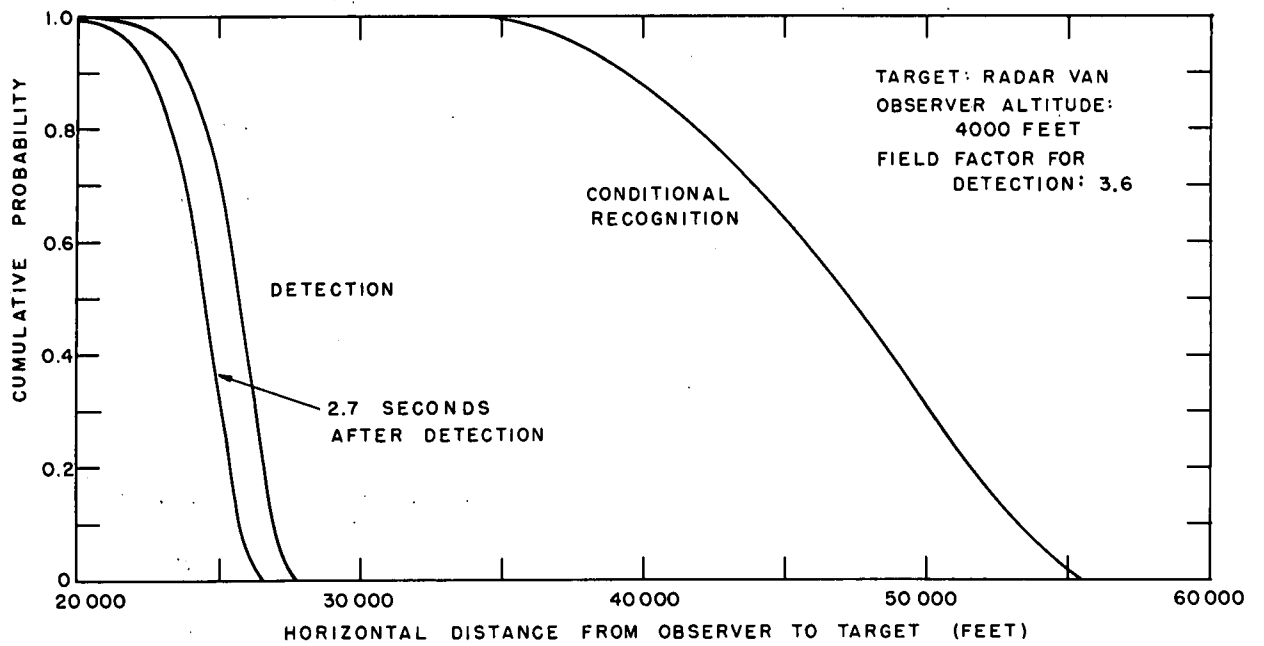


FIGURE 37 - TYPICAL RELATIONSHIP BETWEEN PROBABILITIES OF DETECTION AND CONDITIONAL RECOGNITION

## 5.0 ACKNOWLEDGMENTS

The successful completion of this project was made possible by the efforts of a large number of people both at the Naval Ordnance Test Station and at the Visibility Laboratory. The author wishes to take this opportunity to acknowledge these efforts.

Naval Ordnance Test Station: The project was administered by L. O. Erwin; the camera pod was designed and the aerial photographic coverage arranged by L. Barker. The photographic flights were made by the Naval Air Facility; tracking and communications at "Charlie" Range were handled by D. W. Mack, R. S. McClarry, and Staff. Observer briefing and coordination was by Lt. Cdr. Farren. The observers were from Squadrons VX-5 and VMA-223.

Visibility Laboratory: The technical management of the work was by a committee consisting of S. Q. Duntley, J. L. Harris, J. H. Taylor, and project engineer and author of this report, J. I. Gordon. The ground station during the field experiment was manned by D. M. Webb and C. M. Hansen. Photographic sensitometry was handled by J. C. Brown. Photometric instrumentation and calibration by R. W. Johnson and G. H. Tate. The contributions from the Visual Target Classifier Program and the RADI Program were handled by R. L. Ensminger. Computer programming by A. L. Shaules and M. L. Myers. Photogrammetry and densitometry of aerial films was handled by J. W. Wasserboehr. Data



reduction of goniophotometry and illuminometry was by D. M. Resch. Detection and recognition computations by P. V. Church. The model radar van was made by J. C. Wilds. General assistance was rendered by J. M. Marshall, R. L. Stapleford, C. F. Pinkham, and K. B. MacAdam.

#### 6.0 REFERENCES

1. Summary report covering the field experiment and the predictions is in process and will be issued by Code 12, Naval Ordnance Test Station.
2. A report soon to be prepared on the Visual Target Classifier Program under Bureau of Ships Contracts NObs-72092 and NObs-84075, Assignment 8.
3. J. H. Taylor, "Contrast Thresholds as a Function of Retinal Position and Target Size for the Light-Adapted Eye," University of California, Scripps Institution of Oceanography, Visibility Laboratory, SIO Ref. 61-10, (March 1961).
4. A. Ford, C. T. White, and M. Lichtenstein, "Analysis of Eye Movements During Free Search," J. Opt. Soc. Am. 49, 287-292 (1959).
5. J. L. Harris, "Restoration of Atmospherically Distorted Images," University of California, Scripps Institution of Oceanography, SIO Ref. 63-10, (March 1963).
6. D. R. E. Brown, "Natural Illumination Charts," Bureau of Ships Project NS-714-100, Report No. 374-1 (1952).

7. Kodak "Manual of Physical Properties," Aerial and Special Materials W-40. Kodak Plus X Aerecon Film. Type No. 8401 (March 1963).
8. J. L. Harris, "Optimum Fixation Period for Visual Search," S. Q. Duntley Report No. 3-4, (March 1959), p. 13.
9. H. R. Blackwell, "Contrast Thresholds of the Human Eye," J. Opt. Soc. Am. 36, 624-643 (1946).
10. S. Q. Duntley, "The Functioning Capabilities of Unaided Human Vision in Aerial Reconnaissance," Armed Forces-National Research Council Vision Committee Secretariat, University of Michigan, Ann Arbor, Michigan, (Jan. 1953) Section 5.
11. James L. Harris, "A Possible Criterion for Visual Recognition Thresholds," University of California, Scripps Institution of Oceanography, Visibility Laboratory, SIO Ref. 59-65, (November 1959), p. 17.